

**SURFACTANT/LSW FLOODING IN CARBONATES:
AN INVESTIGATION OF HYBRID EOR METHOD
DESIGN TO IMPROVE OIL DISPLACEMENT**

by

AIDA SAMANOVA

2021

Thesis submitted to the School of Mining and Geosciences of Nazarbayev
University in Partial Fulfillment of the Requirements for the Degree of
Master of Science in Petroleum Engineering

Nazarbayev University
April, 2021

Acknowledgements

Throughout the writing of this thesis, I have received a great deal of support and assistance.

First and foremost, I wish to express my deepest gratitude to my esteemed supervisor, Professor **Peyman Pourafshary** for his valuable suggestions, continuous support during the planning and development of this research work. His immense knowledge and plentiful experience have encouraged me all the time of my academic research.

I would like to extend my special thanks to my co-supervisor, Professor **Muhammad Rehan Hashmet** for sharing expertise, sincere and useful guidance. The meetings with my supervisors were vital in inspiring me and in keeping my progress on schedule. Their willingness to give their time so generously has been very much appreciated.

I am also grateful to the **School of Mining and Geosciences** and all its member's staff for providing me with all the necessary facilities for the research.

I had the great pleasure of working with **Mariam Shakeel and Ruslan Kushekov**, who have always been a major source of unconditional support and help in these very intense academic years.

To conclude, I wish to thank **my family** for their understanding and consistent support.

Originality Statement

I, Aida Samanova, hereby declare that this submission is my own work and to the best of my knowledge it contains no materials previously published or written by another person, or substantial proportions of material which have been accepted for the award of any other degree or diploma at Nazarbayev University or any other educational institution, except where due acknowledgement is made in the thesis.

Any contribution made to the research by others, with whom I have worked at NU or elsewhere is explicitly acknowledged in the thesis.

I also declare that the intellectual content of this thesis is the product of my own work, except to the extent that assistance from others in the project's design and conception or in style, presentation and linguistic expression is acknowledged.

Signed on 31.03.2021

ABSTRACT

Carbonate reservoirs account for over 50% of the world's conventional hydrocarbon reserves. Waterflooding is considered as principle IOR method in carbonates, worldwide. However, the performance of conventional waterflooding needs to be improved, concerning reservoir features. Experimental studies indicate that the efficiency of the waterflooding depends on several properties of injected water, such as ionic composition and salinity. Low-salinity waterflooding (LSWF) is a relatively recent proposed EOR technique that reduces residual oil saturation by changing the wettability to water-wet features and destabilizing oil layers. The underlying mechanisms behind surfactant injection are the abatement of interfacial tension (IFT) between crude oil and brine, wettability alteration, and an increase in the capillary number. Previous studies proved that LSWF with the combination of chemical EOR provides higher incremental oil recovery than either individual technique. Loss of surfactant due to adsorption is considered as an unfavorable phenomenon during flooding which is also affected by the application of the hybrid method.

In this work, the main objective was to design several hybrid EOR coreflooding experiments to analyze the oil displacement performance and oil/brine/chemicals/LSW interactions during the EOR process. The investigation of the effect of alkali (Na_2CO_3) addition on the adsorption of an anionic surfactant on the carbonate surface was targeted as well.

Aqueous stability and phase behavior tests were done to evaluate the interactions of oil/brine/chemicals at temperatures of 25 °C and 80 °C. The optimal alkali concentration and the salinity of the engineered water (EW) were adjusted for the alkali/surfactant solution and crude oil, which provides the desirable middle phase microemulsion. A static adsorption experiment was conducted to evaluate the effect of alkali (Na_2CO_3) on surfactant adsorption. After selecting the best chemical/EW combination, four chemical EOR core floods were designed to study the effect of the hybrid method on the oil displacement and to investigate the effect of a negative salinity gradient design. For the alkali/surfactant flooding, 1% of the alkali (Na_2CO_3) concentration was used. The selected alkali demonstrated a positive effect on anionic surfactant adsorption reduction. Moreover, the alkali contributed to an increase in oil recovery in engineered water alkali/surfactant flooding (EWASF). The best negative salinity gradient flooding case demonstrated higher oil recovery compared to engineered water surfactant flooding (EWSF) as well.

Table of Contents

TABLE OF CONTENTS.....	V
LIST OF FIGURES	VII
LIST OF TABLES.....	IX
1 INTRODUCTION.....	1
1.1 Background.....	1
1.2 Literature Review	3
1.2.1 Wettability in carbonates	3
1.2.2 Mechanisms of Low Salinity Water Flooding in carbonates	4
(i) Wettability alteration	5
(ii) Multicomponent ionic exchange (MIE).....	6
(iii) pH variation and Rock dissolution	6
1.2.3 Surfactant characteristics	7
(i) Critical Micelle Concentration.....	8
(ii) Types of microemulsion	10
(iii) Phase behavior	10
(iv) Solubilization Ratio	12
1.2.4 Surfactants retention	13
1.2.5 Hybrid EOR Method: Surfactant/LSW Flooding	16
(i) Analysis of coreflooding experiments	17
1.2.6 Negative salinity gradient	20
1.3 Problem definition	21
1.4 Objectives of the Thesis	21
1.4.1 Main Objectives	21
1.4.2 Thesis Structure	21
2 METHODOLOGY	23
2.1 Materials.....	23
2.1.1 Core Samples	24
2.1.2 Brine.....	24
2.1.3 Crude oil.....	28
2.1.4 Surfactant	29
2.1.5 Alkali.....	30
2.2 Procedures	30
2.2.1 Brine, surfactant, alkali solutions preparation.....	30

2.2.2	Rock and fluid properties measurements	31
2.2.3	Aqueous stability and phase behavior tests.....	33
2.2.4	Static adsorption test	35
2.2.5	Coreflooding design.....	37
2.2.5	Coreflooding	38
3	RESULTS	40
3.1	Screening of Alkaline/Surfactant solution	40
3.2	Static adsorption test.....	44
3.3	Coreflooding tests	46
4	CONCLUSIONS AND RECOMMENDATIONS	52
5	REFERENCES	53

List of Figures

Figure 1. Oil recovery from spontaneous imbibition of chalks saturated with 6 variations of AN crude oils (Standnes and Austad, 2000)	4
Figure 2. Mechanism of wettability alteration by “MIE” in carbonate reservoirs (Zhang et al., 2006)	6
Figure 3. Definition of the CMC (Lake, 1989)	9
Figure 4. Effect of CMC on IFT (Green and Willhite, 2018)	9
Figure 5. Definition and structure of microemulsion (Healy & Reed, 1974)	10
Figure 6. Microemulsion types and the phase behavior as a function of salinity (Green and Willhite, 2018)	11
Figure 7. Ternary diagrams of phase behavior variation due to salinity effect	12
Figure 8. Impact of salinity to solubilization ratio of water and oil phases (Healy et al. 1976)	13
Figure 9. Effect of salinity on the transmissibility of light of surfactant solution (Somasundaran et al., 1984)	15
Figure 10. The influence of surfactant concentration on the transmissibility of light of solution (Somasundaran et al., 1984)	16
Figure 11. Current stages of implementation of different EOR techniques (Kokal and Al-Kaabi, 2010)	16
Figure 12. Schemes of 4 experiments flooding designs on Berea sandstone cores B1, B2, B3, and B4 (Alagic & Skauge, 2010)	17
Figure 13. Total oil recovery vs injected pore volume for samples B1, B2, B3, B4 (Alagic and Skauge, 2010)	18
Figure 14. Oil recovery, WBT, and dP profile as a function of PV injected for core L1	19
Figure 15. Oil recover (%) vs injected PV	19
Figure 16. Limestone core sample	24
Figure 17. Schematic diagram of salinity design for core flooding experiment #3	27
Figure 18. Schematic diagram of salinity design for core flooding experiment #4	27
Figure 19. Crude oil dynamic, kinematic viscosity, and density versus temperature	29
Figure 20. SVM 3001 Viscometer	31
Figure 21. Manual Saturator (AP-007-001-1) by Vinci-Technologies	32
Figure 22. Aging Cell Apparatus (ACA 700)	33
Figure 23. Schematic illustration of middle phase formation and microemulsion phase transition as a function of salinity	34
Figure 24. Evolution 300 UV-Vis Spectrophotometer	36

Figure 25. Roller oven	36
Figure 26. Phase behavior test at 80 °C for Na ₂ CO ₃ concentrations of 0.25%, 0.5%, 1% and 2%	40
Figure 27. Phase behavior test at 80 °C for Na ₂ CO ₃ concentrations of 1% of the aqueous phase with 1.5, 2, 4, 6 times diluted EW	41
Figure 28. Phase behavior test at 25 °C for Na ₂ CO ₃ concentrations of 0.5%, 0.75%, 1%, 1.25%, 1.5% with 1.5 times diluted EW	42
Figure 29. Phase behavior test at 80 °C for Na ₂ CO ₃ concentrations of 0.5%, 0.75%, 1%, 1.25%, 1.5% with 1.5 times diluted EW	42
Figure 30. Microemulsion ratio of each sample	43
Figure 31. Microemulsion ratio of each sample	43
Figure 32. Aqueous stability test at 25 °C.....	44
Figure 33. Aqueous stability test at 80 °C.....	44
Figure 34. UV absorbance for each surfactant concentration.....	44
Figure 35. Calibration curve	45
Figure 36. Adsorption vs alkali concentration.....	46
Figure 37. EWSF experiment results (dP and oil recovery vs PV injected).....	48
Figure 38.. EWASF experiment results (dP and oil recovery vs PV injected).....	48
Figure 39. RF (%ROIC) for EWSF and EWASF core flooding experiments.....	49
Figure 40. Negative salinity gradient experiment #3 results (dP and oil recovery vs PV injected).....	50
Figure 41. Negative salinity gradient experiment #4 results (dP and oil recovery vs PV injected).....	50
Figure 42. RF (%ROIC) for EWSF, Negative salinity gradient 1 and 2 core flooding experiments	51

List of Tables

Table 1. Parameters of flooding fluids and IFT values (Alagic and Skauge, 2010).....	17
Table 2. Core samples primary measurements	24
Table 3. Chemicals used for brines preparation.....	24
Table 4. Composition of major ions of formation water (Isabaev Y. et. al., 2015).....	25
Table 5. Ionic composition of South Caspian Seawater (Tuzhilkin, et al., 2005)	25
Table 6. Ionic composition of the optimized engineered water (EW).....	26
Table 7. Injection brine composition for core flooding experiment #3	27
Table 8. Injection brine composition for core flooding experiment #4	28
Table 9. Crude oil composition.....	28
Table 10. Anionic surfactant characteristics	29
Table 11. Mass of salts required to prepare different brines.....	30
Table 12. Coreflooding proposed designs	38
Table 13. Phase volumes at 80 °C for Na ₂ CO ₃ concentration of 1% of the aqueous phase with 1.5, 2, 4, 6 times diluted EW.....	41
Table 14. Calibration curve values	45
Table 15. Adsorption density	45
Table 16. Coreflooding experiment details.....	46
Table 17. RF for EWSF and EWASF experiment results	48
Table 18. RF for Negative salinity gradient experiments	50

1. Introduction

1.1 Background

There are three production phases of hydrocarbon extraction from the subsurface, known as primary, secondary, and tertiary. The selection of a production stage for reservoir development depends on formation fluid properties, reservoir drive mechanisms, reservoir properties, well communication, and the level of risk in investment, i.e., understanding reservoir behavior from a historical record of inputs and outputs. At the primary recovery stage, the hydrocarbon is produced by natural sources of energy, such as the expansion of reservoir fluids (oil and gas), aquifer drive, and formation expansion. The total recovery may reach 10-25% of original oil in place (OIIIP). Therefore, artificial reservoir pressure supports are needed to be applied to increase the recovery. At the secondary production phase, mainly gas or water-flooding methods are used. However, after reservoir pressure maintenance, a significant part of the hydrocarbon is either bypassed or still trapped in small pores. In that case, the tertiary recovery or enhanced oil recovery (EOR) methods can be helpful for the mobilization of the trapped oil. EOR reduces the residual oil saturation and, depending on the field development plan, can increase or decrease the reservoir life by modifying the chemical and physical parameters of injected fluids. The method of displacement efficiency improvement of the oil depends on several factors, such as reservoir properties, project cost, availability of the resources, and technology.

Over 50% of the proven conventional hydrocarbon reserves are in carbonate reservoirs. The average recovery factor in carbonate formation is below 35% due to the complex structures, formation heterogeneities, and oil-wet/mixed wet conditions resulting from their depositional history and later diagenesis (Abdallah et al., 2007). However, there is a high potential to increase oil recovery in carbonate reservoirs by using EOR methods.

The majority of carbonate field development plans that improve oil recovery by water and gas flooding that still do not provide high ultimate recovery. The performance of conventional waterflooding needs to be enhanced further considering reservoir features. Experimental studies and field experiences indicate that the efficiency of the waterflooding depends on the salinity and composition of the injected water. Low salinity waterflooding (LSWF) is a relatively recent and promising EOR technique. Low salinity water can be obtained through dilution of high saline seawater or formation water and optimization of the active ions (such as

Ca²⁺, Mg²⁺, and SO₄²⁻) (Al-Shalabi & Sepehrnoori, 2015; Hosseini et al., 2020). Low salinity waterflooding may alter the wettability of carbonates toward the water-wet condition through proposed mechanisms such as multicomponent ionic exchange (MIE) and double layer expansion (Zhang & Morrow, 2006; Fathi et al., 2011; Esene et al., 2018).

Surfactant flooding (SF) is a chemical EOR method that provides IFT reduction and wettability alteration (Sheng, 2015). Surfactant flooding, together with LSWF, is a new, promising hybrid method of EOR (Araz & Kamiyabi, 2015). In past years, the application of surfactants with the integration of LSWF has acquired widespread interest among researchers. Most of the studies focus on sandstone formations. LSWF and SF experiments were done in carbonates separately, and few research studies attempted to utilize this hybrid combination in carbonates together.

The success of this method depends on several factors that are discussed in this work. High incremental oil recovery and low retention of surfactant, which decreases the project cost, are the leading indicators of the effective hybrid injection process. High oil recoveries from the porous medium can be attained at a high capillary number due to the ultralow IFT values (Lake, 1989). Surfactants that provide better IFT reduction at low salinity conditions are more accessible and more cost-effective than those that are practical in high salinity water. Besides, surfactant retention intensifies as salinity increases (Ahmed and Elraies, 2018). Alagic and Skauge (2010) reported a hybrid EOR project combining the influence of low salinity (LS) brine and surfactant flooding in a combined low salinity brine and surfactant (LSS) flooding process. The concept of this hybrid EOR method is that during LSWF, oil layers destabilize in a low IFT condition, which is provided by SF that also prevents re-trapping. Alameri et al. (2015) reported an increase in incremental oil recovery by more than 10% after the injection of LSS into carbonate core samples (Alameri et al., 2015).

It is believed that carbonates are not suitable for anionic surfactant flooding due to the presence of positively charged rock surfaces and the high adsorption of negatively charged anionic surfactants. By application of alkaline and shifting the pH to values above 9, the surface charge of carbonates surface may change (Zhang et al., 2006), and the adsorption is controlled. Hence, by this new design, the application of anionic surfactant can be considered as a cheaper and more practical option in a hybrid injection scheme.

1.2 Literature Review

1.2.1 Wettability in carbonates

Wettability is one of the essential reservoir properties for consideration in the design and execution of reservoir development plans. Wettability influences microscopic displacement in porous media, capillary pressure (P_c), and the relative permeability of oil, gas, and water phases, which in turn has an impact on multiphase fluid flow (Strand et al., 2006). Therefore, investigation of the wetting condition of reservoir rock has a significant role, as it influences the oil recovery. More than half of hydrocarbon reserves are trapped in carbonate reservoirs, particularly in limestones and dolomites. Traditionally, primary oil recovery from carbonates is lower than 30% due to the mixed or oil-wet character, heterogeneity, low permeability, and natural fractures. Carbonates are composed of different minerals that have variations in wetting properties. However, the main constituents of reservoirs — quartz, limestone, and dolomite are typically water-wet before the oil migrates to the reservoir (Wood & Yuan, 2018). Several factors may affect carbonate wettability behavior, such as surface electrical charge, acid and base numbers of crude oil, temperature, pressure, and the composition of formation water (Strand et. al., 2006; Hiorth et. al., 2010).

Acid number (AN, mg KOH/g) is a significant wetting indicator of the crude oil/brine/rock (CBR) system that represents the amount of carboxylic material in crude oil. As a rule, the carbonate surface is positively charged, and the carboxylic group, $-\text{COO}-$, with a negative charge, provides a strong bond to the rock. The carboxylic group can commonly be found in the heavy polar fraction of crude oil (Speight, 1999). Buckley et al. (1995) also confirmed that the wettability of rock can be altered due to the adsorption of asphaltene and resin fractions from crude oil on the rock surface. The results of spontaneous imbibition tests are demonstrated in Figure 1, where 6 oil samples with different AN were used. An increase in AN makes the system more oil-wet, which reduces the oil recovery (Standnes and Austad, 2000).

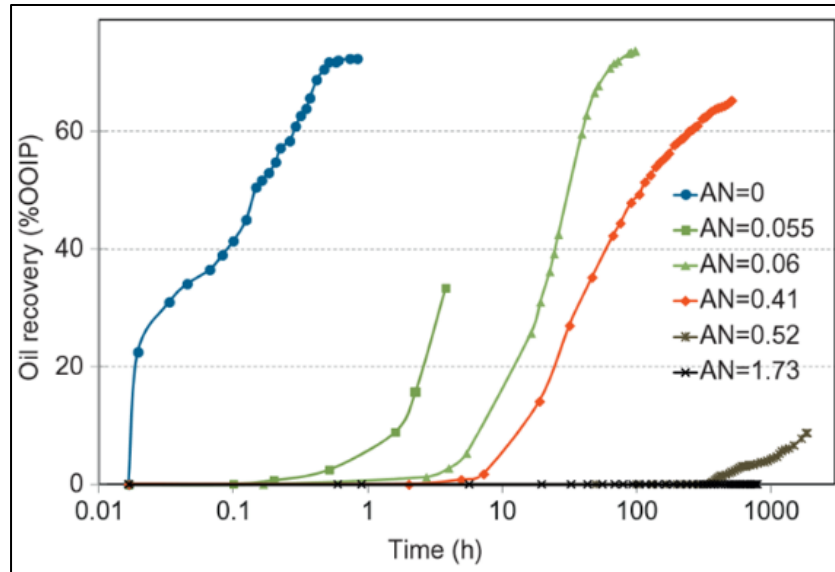


Figure 1. Oil recovery from spontaneous imbibition of chalks saturated with 6 variations of AN crude oils (Standnes and Austad, 2000)

The other parameter that affects the wettability is the base number (BN, mg KOH/g). The high value of BN can attenuate the influence of acidic material and can contribute to more water-wet conditions for chalk (Puntervold et al., 2007). At high temperatures, the AN of the crude oil tends to be low due to the high decarboxylation of the acidic group, where solid CaCO_3 catalyzes that process (Shimoyama and Johns, 1972). Hence, the temperature is a critical parameter, which in high values turns the carbonate rock to a more water-wet state (Rao, 1996). Wettability properties may also be affected by the composition of the formation water. Sulfate is the most active ion in carbonates concerning wetting properties. Commonly, the quantity of sulfate (SO_4^{2-}) in formation water is low due to anhydrate precipitation (CaSO_4), which occurs because of the high concentration of Ca^{2+} cations in formation water at high reservoir temperature of reservoirs. As a result, the rock becomes more water wet with the participation of sulfate ions in the formation brine (Shariatpanahi et al., 2011., Shariatpanahi et al., 2016).

Wettability alteration is an effective approach during the chemical EOR process, as it increases oil recovery. The purpose is to change rock wettability from oil-wet to water-wet conditions. Several studies indicated that both LSWF and SF provide wettability alteration of rock surfaces (Chen et al., 2006; Falode & Manuel, 2014). This point shows the possibility of designing a new hybrid method to use the benefits of both approaches in EOR.

1.2.2 Mechanisms of Low Salinity Water Flooding in carbonates

LSWF is one of the easiest to deploy and the most cost-effective methods of increasing oil recovery from a reservoir. In literature, low salinity water (LSW) is mentioned as engineered

water (EW), and smart water as well. It is believed that a change in wetting properties is the main reason for the occurrence of low salinity effects (Araz and Kamyabi, 2015). Different mechanisms are proposed to explain the oil recovery by LSWF for both sandstones and carbonates, such as fines migration, multicomponent ionic exchange (MIE), interfacial tension (IFT) reduction, electric double-layer expansion, mineral dissolution, capillary pressure reduction, pH variation, and wettability alteration. As a result of the integration of mechanisms mentioned above, the wettability of rock modifies from mixed-wet and oil-wet to water-wet conditions. Consequently, residual oil saturation reduces, and the total oil recovery increases due to the improvement of the microscopic displacement efficiency. LSWF has comparatively low operating and capital cost (McGuire et al., 2005; Yousef et al., 2012). Another feature of LSWF is the applicability in the early stages of oil production as well as in the late life cycle of the fields (Yousef et al., 2012; Kazankapov, 2014). There is an opportunity to use LSWF with other chemical and thermal EOR methods.

The application of low salinity surfactant flooding (LSSF) in sandstones was studied more extensively compared to carbonates due to the belief that the presence of clay improves the effect of LSWF (Al-Shalabi & Sepehrnoori, 2016). Yousef and colleagues (2012) reported successful LSWF coreflooding and field trials in carbonates. The improvements in oil recovery in carbonates by using LSWF were outlined by Webb et al. (2004); Ligthelm et al. (2009); Puntervold et al. (2009); Yosef et al. (2011). However, there are a few failure cases reported by Fathi et al., (2010), when a reduction in oil recovery for chalk cores was noted.

(i) *Wettability alteration*

The mechanism depends on the integrity of the water film, which occurs between the rock surface and liquid. From the attractive interaction of two phases, disjoining pressure phenomena arises. It is caused by interionic forces (van der Waals and electrostatic forces) that create repulsive disjoining pressure. As a result, the water film stabilizes, whereas the stability depends on brine pH, the composition of crude oil, salinity, and reservoir temperature (Katende et al., 2019). When salinity increases, the electrostatic repulsion decreases, which weakens film stability. Wettability alteration that was observed during LSWF was announced in numerous studies. Several studies were conducted where carbonate rock samples from Ekofisk, Valhall, Yates fields were used to study spontaneous imbibition tests in oil-wet rocks. They concluded that the presence of SO_4^{2-} promoted spontaneous imbibition (Awolayo et al., 2018). Wettability

alteration in carbonate rocks can occur when the LSWF contains Ca^{2+} or/and Mg^{2+} at high temperatures (above 90°C) (McMillan, 2016).

(ii) Multicomponent ionic exchange (MIE)

Oil-wet features of the carbonates can be changed toward water-wet conditions due to a multicomponent ionic exchange (MIE) mechanism (Zhang et al., 2006; Austad et al., 2009). This proposed mechanism involves the interaction of Ca^{2+} , Mg^{2+} , SO_4^{2-} ions with the rock and crude oil. Negatively charged sulfate (SO_4^{2-}) ions react with the calcite surface, lowering its positive surface charge. As a result, calcium ions (Ca^{2+}) move closer to the rock surface due to the electrostatic repulsive force reduction. Ca^{2+} reacts with negatively charged carboxylic material and detaches it from the rock surface (Zhang et al., 2007), as shown in Figure 2. The adsorption of sulfate (SO_4^{2-}) and calcium (Ca^{2+}) ions intensify with increasing temperature. The Mg^{2+} ions also start to substitute Ca^{2+} ions intensely with increasing the temperature (Strand et al., 2006).

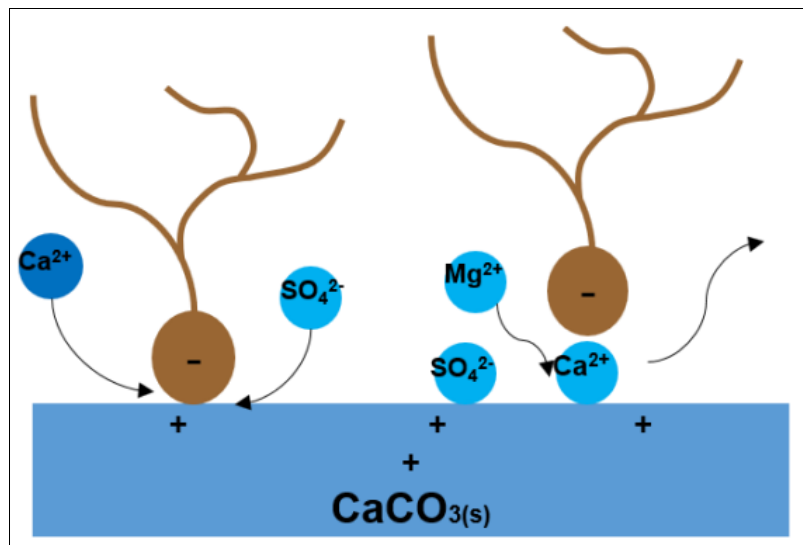
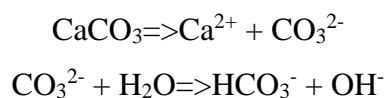


Figure 2. Mechanism of wettability alteration by “MIE” in carbonate reservoirs (Zhang et al., 2006)

(iii) pH variation and Rock dissolution

Multiple observations showed rising pH, mostly because of the cation exchange or dissolution of carbonates. The following carbonate dissolution reactions show that the dissolution increases the pH of the produced solution (Altair & Hussein, 2017).



Some experiments showed that if pH is low at the beginning, the recent changes resulted in better effects. Sometimes oil recovery rises independently of pH alteration. Austad et al. (2010) experimentally observed that an increase in pH and wettability alteration occurred due to reaction between H^+ from the liquid phase and divalent cations. McGuire et al. (2005) found out that low salinity water starts to act analogously to alkaline flooding when pH is boosted; alkalines, in turn, can produce surfactants in-situ. Hiorth et al. (2008) reported the dissolution of calcite as a key mechanism that causes wettability alteration in carbonates. According to this study, calcium (Ca^{2+}) ions react with the sulfate (SO_4^{2-}) ions causing anhydrate precipitation at high temperatures. After the reaction with the rock surface, the extra calcium (Ca^{2+}) ions move closer to the surface and detach the oil.

1.2.3 Surfactant characteristics

Surfactants or surface acting agents are amphiphilic organic compounds that are soluble in both water and organic solvent. Surfactants consist of a hydrocarbon (non-polar) chain, which is also called a hydrophobic tail, and a polar or ionic portion, which can be simplified as a hydrophilic head (Sheng, 2011). The hydrophobic tail interacts with an organic solvent, and the hydrophilic head part interacts with water. This process leads to the formation of oil-in-water and water-in-oil microemulsions, which depends on the balance between the lipophilic and hydrophilic groups of a surfactant (Alagic, 2010). Surfactants may be classified based on the role in the EOR process as primary surfactants or cosurfactants. Cosurfactants help to accelerate the surfactant action that forms microemulsion directly by altering the surface energy and the viscosity of liquids. Moreover, cosurfactants change the packing density at interfaces and break up liquid crystals. (Green and Willhite, 2018).

There are four groups of surfactants as anionic, cationic, nonionic, and zwitterionic that are categorized concerning the ionic nature of the head group (Ottewill, 1984). Anionic surfactants have a negatively charged head part that leads to the less adsorption on negatively charged clay, thus it is mostly applicable for sandstones (Zolotukhin and Ursin, 2000). The other reasons for anionic surfactant prevalence are economic feasibility, effectiveness in IFT reduction, and relative stability.

In an aqueous solution, after the ionization process, the cationic surfactant head part has a positive charge. Hence, the cationic type of surfactants is functional in carbonates due to the low adsorption on the rock surface. Furthermore, the reason for the broad utility of cationic

surfactants in carbonates is wettability alteration from oil-wet to more water-wet behavior and reduction in the loss of surfactant (Mwangi, 2010).

Nonionic surfactants are neutral; hence, there is no charge on the head portion, and they have a larger head compared to the tail. The advantages of nonionic surfactants are stability in high saline environments and the ability to improve the phase behavior of the system as a cosurfactant (Sheng, 2011). The main drawback of nonionic surfactants is the weak IFT reduction capacity; for that reason, it is used in combination with anionic surfactants, which makes the mixture persistent to salinity.

Amphoteric or zwitterionic surfactants consist of dual charged groups: nonionic-cationic, or anionic-cationic, nonionic-anionic, nonionic-cationic. Mostly, the overall charge and reaction of zwitterionic surfactants depend on the pH of the solution (Lake, 1989). Thus, in acidic solution, zwitterionic surfactants acquire cationic surfactant behavior, and in alkaline solutions, they react as anionic surfactants. As advantages, they exhibit strong tolerance to high temperatures and high salinities.

Moreover, in combination with the surfactant, cosurfactants are added to the solution to improve microemulsion properties (Zhou and Rhue, 2000). Cosurfactants provide a reduction in surfactant precipitation by solubility initiation, improvement in IFT, viscosity variation of the microemulsion, added mobility in the movement of hydrocarbon tail, and modification of hydrophilic-lipophilic balance (HLB) (Comelles and Pascual, 1997).

(i) Critical Micelle Concentration

Critical Micelle Concentration (CMC) is an important parameter that are used to characterize the surfactants. It can be specified as the threshold concentration of surfactants, after which micelles begin to form. Figure 3 shows the behavior of surfactant monomer concentration versus total surfactant concentration. According to the curve, after reaching the CMC, the surfactant monomer concentration remains constant, but micelles concentration increases. The high concentration of micelles obstructs the further reduction of free energy of the system. At the time the surfactant solution interacts with the oleic phase, the surfactants start to build up in the transitional interface. The hydrophilic part dissolves in the water phase, and the lipophilic portion goes to the oleic phase. The surfactant accumulates at the interface between the water and oil. Low surfactant concentration is required to fill the interface and reduce the IFT between oil and water.

The IFT between oil and surfactant solution depends on the salinity, temperature, surfactant type, surfactant concentration and oil composition (Green & Willhite, 2018). Figure 4 shows the IFT behavior as a function of surfactant concentration. There is a sharp decrease in IFT when surfactant concentration is increasing until the CMC is reached. After this point, only a negligible change in IFT is noticed. It can be explained by the micelles formulation that was created from the excess surfactants. These additional surfactants do not increase the surfactant concentration at the water/oil interface.

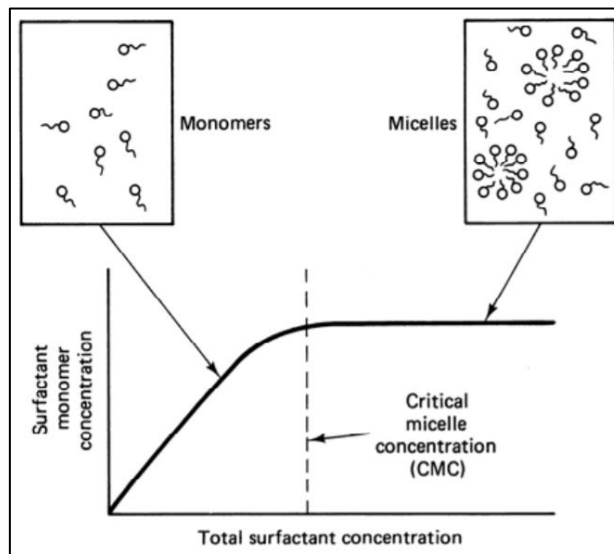


Figure 3. Definition of the CMC (Lake, 1989)

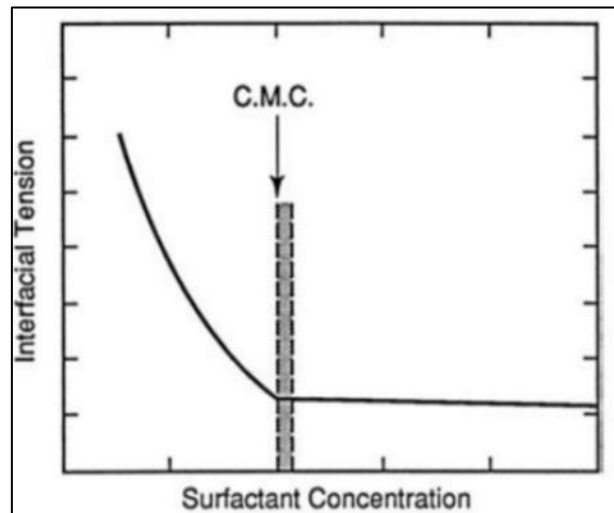


Figure 4. Effect of CMC on IFT (Green and Willhite, 2018)

(ii) Types of microemulsion

Microemulsions or swollen micelles are formed when micelles solubilize a phase that is immiscible with the solution. The microemulsion formation is a widespread EOR technique that provides IFT reduction and increases the oil recovery due to a reduction in residual oil saturation (Santanna et al. 2009; Bera et al. 2014). It is a transparent (translucent) homogeneous solution of water and hydrocarbons with a high concentration of surfactant (Stoeckenius et al., 1960). Microemulsions look cloudy when dark viscous oil is used, as it consists of aggregated micelles (Meyers and Salter, 1981). The size of swollen micelles is larger than micelles that have not solubilized and have a range from 10-200 μm . In an aqueous solution, the microemulsion is transparent or semi-transparent regardless of the amount of solubilized hydrocarbon in the micellar solution. The opposite term for microemulsion is macroemulsion, which has a larger size of particles, and the solution is opaque and cloudy. Macroemulsions are not thermodynamically stable like microemulsions but may persist for a long time.

Based on the continuous phase, the microemulsion can be classified as hydrocarbon-external, water-external, or lamellar (intermediate) type, as shown in Figure 5. Those configurations depend on the oil/water ratio, surfactant parameters, and temperature. Lower phase microemulsion occurs when microemulsion is the aqueous phase that accumulates below the oleic phase due to higher density than the oleic phase. At high salinity conditions, the microemulsion is an oil-external type and has an excess water phase, which means it is an upper-phase microemulsion. Sometimes the system may have excess water, excess microemulsion, and excess oil phases due to intermediate salinity ranges. This configuration is called a middle phase microemulsion (Healy et al., 1976).

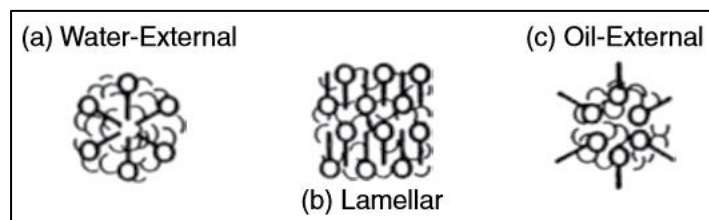


Figure 5. Definition and structure of microemulsion (Healy & Reed, 1976)

(iii) Phase behavior

The phase behavior of a surfactant solution is a complicated term that is controlled by a variety of factors: brine salinity, temperature, concentration, and type of surfactants, cosurfactants, hydrocarbons, and pressure. Phase behavior of microemulsions is measured innovatively, so it

has no universal equation. It can be presented with the help of a ternary diagram and empirical correlations.

The salinity of the water has an impact on the phase behavior of the surfactant solution. The solubility of anionic surfactant in water becomes lower when the salinity of formation water increases. Surfactants start to move from the water phase to the oil phase as the electrolyte concentration becomes high. Hence, when the salinity of brine increases, the surfactants go to the oleic phase from the aqueous phase, as illustrated in Figure 6.

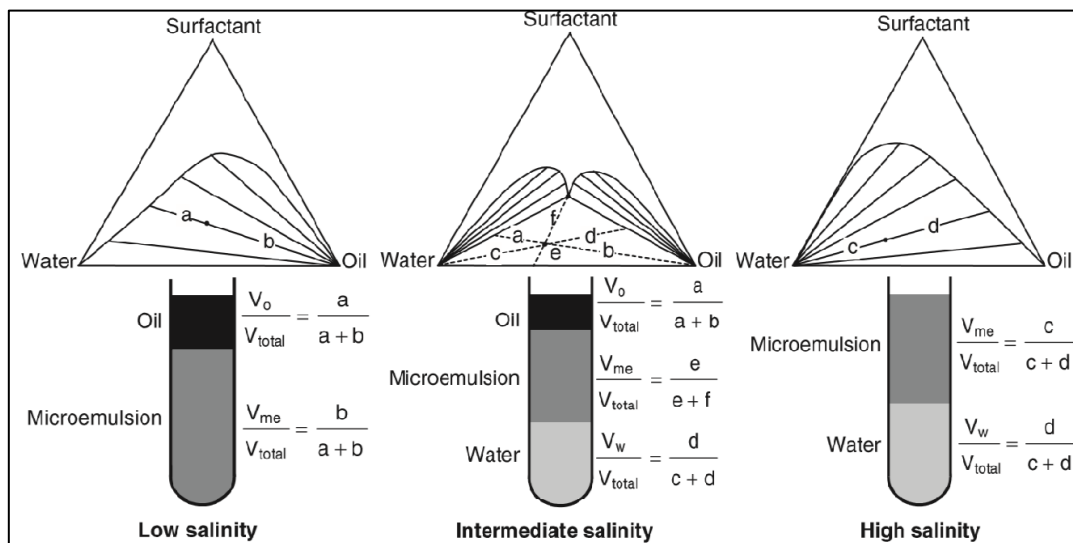


Figure 6. Microemulsion types and the phase behavior as a function of salinity (Green and Willhite, 2018)

- Figure 6 demonstrates oil-surfactant-water phase behavior in a ternary diagram considering the salinity of the system. Winsor divided microemulsions into types I, II, III, and IV. The single-phase area above the multiphase region, where the concentration of surfactant is high, is denoted as type IV microemulsion. However, suggested numbers aren't equivalent to the number of presented phases that complicates the link with the microemulsion characteristics.
- Lower-phase microemulsion: Type II(-) microemulsion; Winsor Type I microemulsion; water-external microemulsion. When the top of the ternary diagram corresponds to 100% surfactant, the lower right side represents the oil, and the lower-left represents the water, the tie lines have a negative slope, and there are two phases.
- Middle-phase microemulsion: Type III microemulsion; Winsor Type III microemulsion; bicontinuous microemulsion. Notably, that 3-phase region is the favourable case, due to ultralow IFT between water and oil phases. According to Winsor, these microemulsions, that are in equilibrium with oil and water.

- Upper-phase microemulsion: Type II(+) microemulsion; Winsor Type II microemulsion; oil-external microemulsion. In the case of identical placement of elements, the tie lines have a positive slope, and there are also two phases. (Nelson and Pope, 1978).

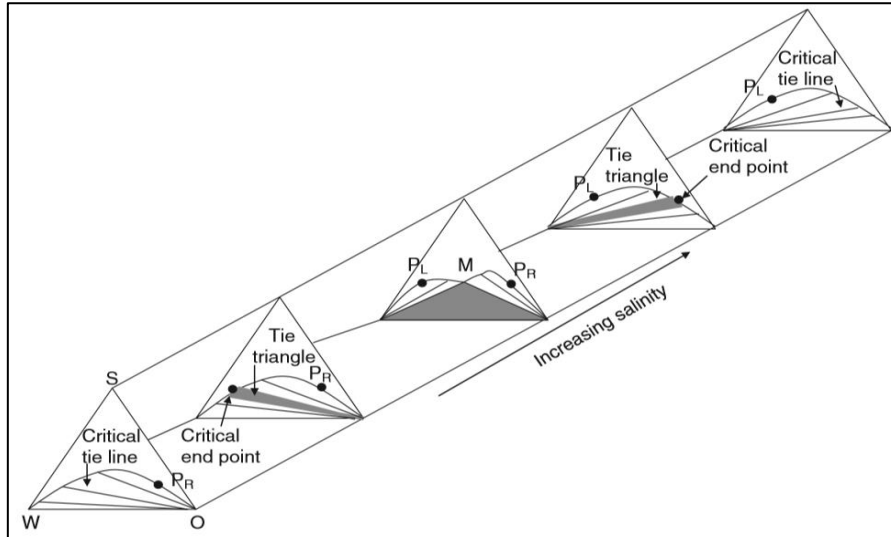


Figure 7. Ternary diagrams of phase behavior variation due to salinity effect

where, M = Middle phase microemulsion, P_L = Plait point on the left, P_R = Plait point on the right. As Figure 7 reveals, the conversion from Type II(-) to Type II(+), or in the opposite direction, every time takes place through the Type III environment.

(iv) Solubilization Ratio

Terms such as solubilization ratio, R-ratio, and packing factor show solution phase behavior. The value that indicates the ratio of the solubilized volume of brine or oil to the volume of surfactant is called the solubilization ratio and can be calculated by equation 1.2.3.c and 1.2.3.d.

$$\delta_w = \frac{V_w}{V_{surf}} \quad 1.2.3.c$$

$$\delta_o = \frac{V_o}{V_{surf}} \quad 1.2.3.d$$

where δ_w is the water solubilization ratio, V_w is the volume of water solubilized in the microemulsion, V_{surf} is the volume of surfactant in the microemulsion, δ_o is the oil solubilization ratio, V_o is the volume of oil solubilized in the microemulsion.

There is a theoretical relation between IFT and solubilization ratio suggested by Huh in 1979, as shown in the Equation 1.2.3.e below:

$$\sigma = \frac{C}{\delta^2} \quad 1.2.3. e$$

where σ is the IFT, δ is the optimum solubilization ratio, and C is the constant ~ 0.3 dynes/cm for crude oil. In the case with the optimum solubilization ratio greater than 10, the IFT is approximately less or equal to 10^{-3} dynes/cm. In optimal salinity, the equivalent amount of water and oil are dissolved in Winsor type III microemulsion that indicates the optimum solubilization ratio (Healy, Reed, Stenmark, 1976).

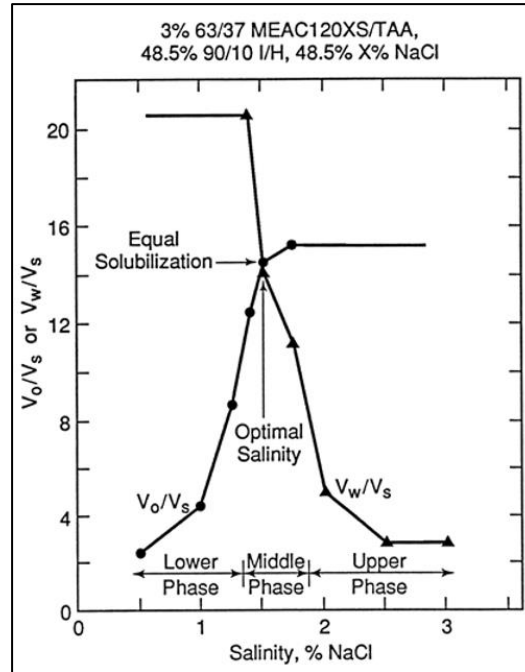


Figure 8. Impact of salinity to solubilization ratio of water and oil phases (Healy et al. 1976)

The dependence of solubilization ratios on salinity is shown in Figure 8. For an experiment, anionic surfactant and monoethanolamine salts of alkylorthoxylene sulfonic acid (MEACNOXS) were used. The used oil was a mixture of 10 % of aromatic oil (N) and 90% of paraffinic oil (I). At optimal salinity, the equal solubilization of phases occurs, and the IFT of the system reaches the ultralow value; as a result, the residual oil recovery has the highest value (Green and Willhite, 2018).

1.2.4 Surfactants retention

Surfactant loss has a negative effect on the feasibility of a surfactant flooding process and increases the required amount of chemicals for a successful EOR method (Novosad, 1981). The reasons for surfactant loss are adsorption, phase trapping, and precipitation processes that lead to low displacement efficiency of hydrocarbon (Ziegler & Handy, 1981). Adsorption depends on fluid and rock surface interaction and takes place when negatively charged

sandstone attracts positively charged cationic surfactants or positively charged carbonates acts with anionic surfactants. Adsorption of surfactants on the rock surface cannot be totally eliminated but can be significantly minimized by increasing the pH of the system. The pH of the electrically neutral charge of the molecule is called isoelectric point (IEP), and for calcite, the value is equal to 9. For silica, the IEP is 2 (Somasundaran and Agra, 1967; Al-Yousef, 1995). Rock surfaces have a negative charge when pH is above the isoelectric point and vice versa for a positively charged surface (Green & Willhite, 2018).

The surfactant may adsorb on the rock surface because of the electrostatic interaction between the surfactant and rock (Kamal et al. 2017). The surface charge of carbonates makes the selection of appropriate surfactant type difficult. Generally, carbonates are positively charged; hence, suitable surfactants are the negatively charged anionic type. Opposite charges on rock and surfactant lead to a decrease in electrostatic interactions between them, that's why surfactant adsorption can also be minimized. If the rock is not pure carbonate, then cationic surfactant may have high retention (Kun Ma et al., 2013).

Kun Ma et al. (2013) investigated the adsorption of the cationic surfactant (CPC) and the anionic surfactant (SDS) on carbonates. The study showed that CPC demonstrated low adsorption on a synthetic calcite surface but high adsorption on natural carbonate surfaces. Adsorption of anionic surfactants can be minimized with the addition of an alkali (Nelson et al., 1984; Wang et al., 1997; Zhang et al., 2000).

There is also a possibility to avoid phase trapping and precipitation of surfactants by regulation of temperature and salinity. The main mechanism for the adsorption is van der Waals and electrostatic interaction between mineral surface and hydrophobic tail of surfactant. Surfactant retention is required to be less than 1 mg/g of rock to be feasible and economic. Experiments have proven that for Berea sandstone, the value of surfactant retention varies from 0.01 to 0.37 mg/g-rock (Lake, 1989). The value of retention depends on the mineralogy of the rock, salinity, pH, surfactant and microemulsion characteristics, and oil properties (Zhang and Hirasaki, 2006; Liu et al., 2010; Solairaj et al., 2012). Retention leads to high IFT and a reduction in the efficiency of the chemical slug (Kamal et al., 2017). Commonly, it is difficult to test in what way surfactant retention has occurred (Trushenski et al., 1974).

One of the reasons for surfactant precipitation is the presence of multivalent ions, which causes the active surfactant and cosurfactant phase dissociation (Meyers and Salter, 1981). Light transmission is one of the methods used to determine the effect of salt, surfactant concentration,

and ion types on surfactant precipitation (Somasundaran et al., 1984). Precipitation and turbidity of solution can be noticed from the decreasing trend of transmissibility of light through the solution, as shown in Figures 9 and Figures 10. In this study, a sodium dodecylbenzene sulfonate (NaDDBS), a sodium benzenesulfonate, and brines with K^+ , Ca^{2+} , Al^{3+} ions were utilized. In Figure 9, the concentration of KCl increases, and when it reaches 0.5 kmol/m^3 , it leads to precipitation, where light transmission respectively suddenly reduces. As a result, an increase in salinity causes a decrease in the surfactant solubility.

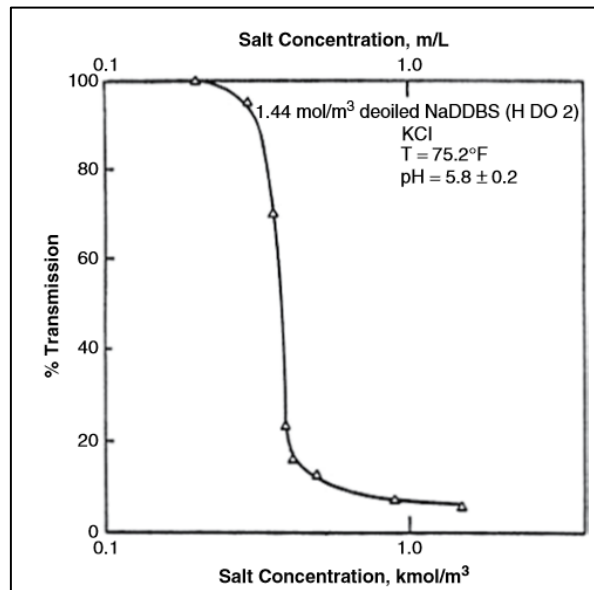


Figure 9. Effect of salinity on the transmissibility of light of surfactant solution (Somasundaran et al., 1984)

Figure 10 shows the change of light transmission for different ions and concentrations. The precipitation of the surfactant takes place at lower concentrations of Al^{3+} ion compared to Ca^{2+} and K^+ ions. Also, when the surfactant (NaDDBS) concentration becomes higher than 10^{-5} kmol/m^3 , it starts to precipitate actively. But when surfactant concentration is above $5 \times 10^{-3} \text{ kmol/m}^3$, it dissolves again. The same scenario happens for divalent and multivalent ions. Appropriate alcohol cosurfactant type helps to solubilize the surfactant solution (Novosad, 1981).

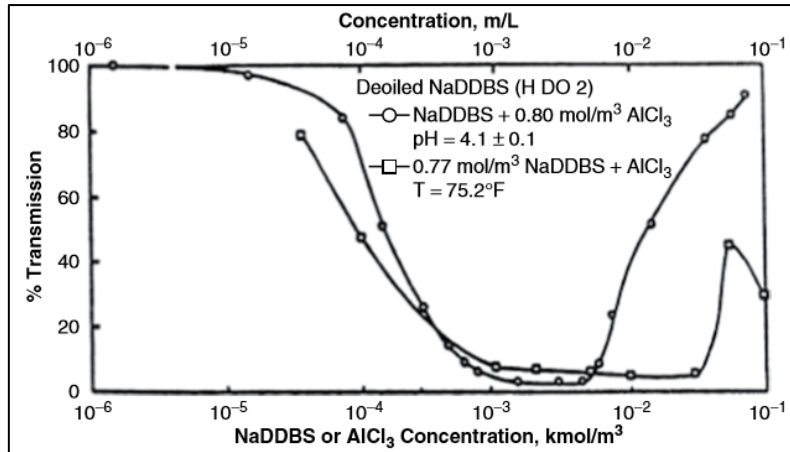


Figure 10. The influence of surfactant concentration on the transmissibility of light of solution (Somasundaran et al., 1984)

1.2.5 Hybrid EOR Method: Surfactant/LSW Flooding

Hybrid EOR methods target to recover more residual oil in an economic, ecological, and technically feasible way by stimulation of multiple mechanisms simultaneously. LSWF promotes a suitable environment for effective surfactant flooding due to the detachment of oil molecules, wettability alteration, and reduction in IFT (Pourafshary and Moradpour, 2019). Moreover, the combination of LSWF with surfactant flooding leads to the minimization of surfactant consumption and improves its solubility and stability, which in turn reduces the project cost. Those are reasons for the priority of hybrid over the single EOR technique. Figure 11 represents the place of hybrid EOR in the research and development stage, which proves its immaturity and need for further investigation (Kokal and Al-Kaabi, 2010).

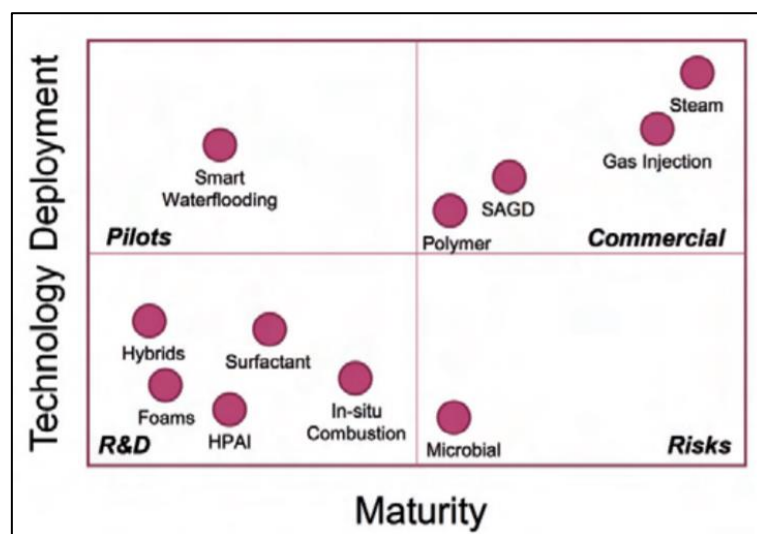


Figure 11. Current stages of implementation of different EOR techniques (Kokal and Al-Kaabi, 2010)

(i) Analysis of coreflooding experiments

Several works stated high tertiary oil recovery by surfactant flooding after LSWF in sandstones and carbonates. According to a study conducted by Alagic and Skauge (2010), the change to LSW of 0.5% NaCl from seawater (SW) of 36000 ppm TDS with anionic surfactant flooding resulted in extra oil recovery by almost six saturation units. Figure 12 presents flooding designs to test the advantages of LSW with the integration of surfactant flooding and the effect of the high pH of the injected water. Core flooding experiments were done on 4 mixed-wet Berea sandstone cores.

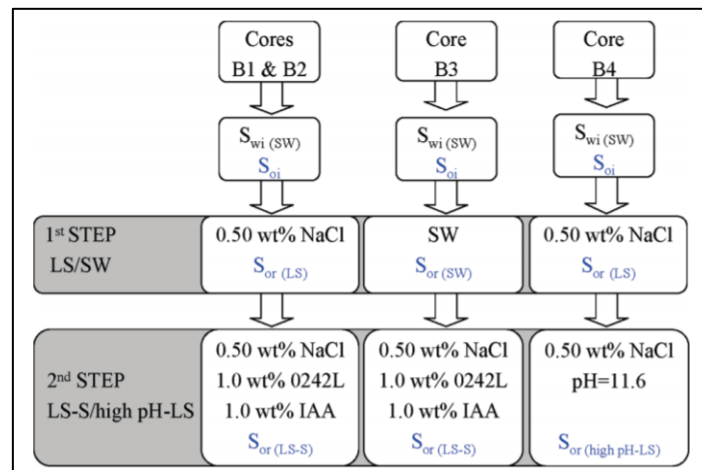


Figure 12. Schemes of 4 experiments flooding designs on Berea sandstone cores B1, B2, B3, and B4 (Alagic &Skauge, 2010)

The research proves retarded water breakthrough (WBT), wettability alteration, and increase in capillary number due to an intensive IFT reduction by the combined effect of high pH LSW and surfactant flooding as demonstrated in Table 1 and Figure 13.

Table 1. Parameters of flooding fluids and IFT values (Alagic and Skauge, 2010)

Fluid type	μ (cp)	IFT (mN/m)
Sea-water	1.15	23.5
Low salinity water	1.01	16.5
LS-SF (pH 11.6)	1.74	1.24×10^{-2}
LS-SF (pH 7.0)		1.71×10^{-2}
Low salinity water with high pH	1.01	1.8

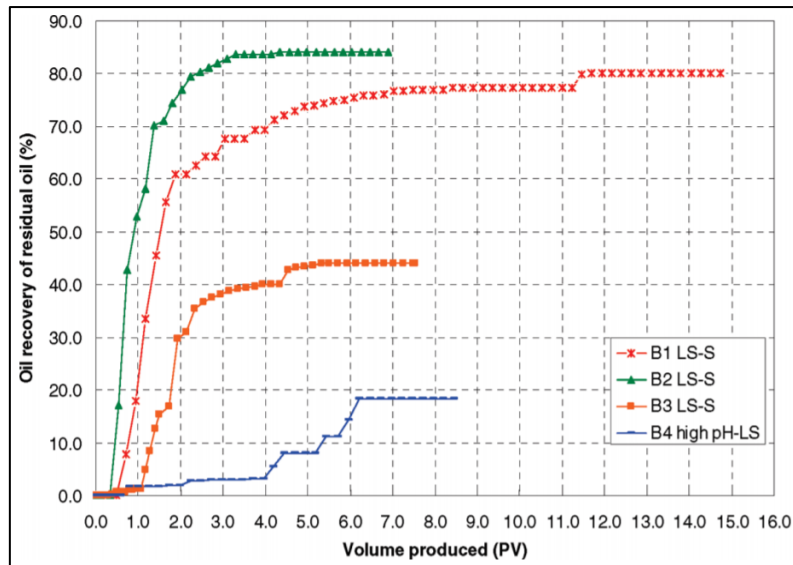


Figure 13. Total oil recovery vs injected pore volume for samples B1, B2, B3, B4 (Alagic and Skauge, 2010)

One of the advantages of this study was the analysis of effluent ions that provided information about the ion retention in cores. As a result, a low concentration of Mg^{2+} shows strong retention on the mineral surface, and a high concentration of Ca^{2+} specifies the dissolution of minerals.

Numerous experiments have confirmed the additional recovery of hydrocarbons from sandstone and carbonate reservoirs due to the application of the hybrid technique. For instance, Alameri et al. (2015) declared more than 10% of tertiary oil recovery in carbonates and Shaddel (2012) observed an additional 5-7% from sandstone core samples by using sodium dodecylbenzene sulfonate surfactant (SDBS) with LSW. The experiment conducted by Khanamiri et al. (2016) on sandstone cores resulted in 2-6% of the additional oil production. Alagic et al. (2011) determined the high effectiveness of the application of LSW and surfactant flooding for oil-wet sandstone core samples. Johannessen & Spildo (2013) conducted laboratory coreflooding experiments to investigate the synergy of LSWF and LSSF in sandstone samples. Figure 14 demonstrates the coreflooding performance for the core L1. LSWF resulted in an additional 7%. Also, the work provides an analysis of the static and dynamic adsorption of surfactant on sandstone surface., IFT measurements and dispersion test.

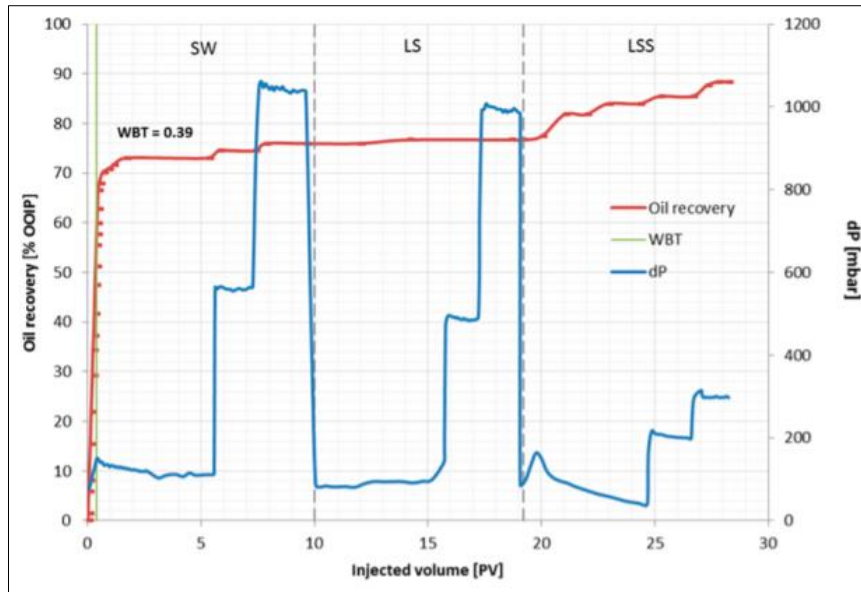


Figure 14. Oil recovery, WBT, and dP profile as a function of PV injected for core L1 (Johannessen and Spildo, 2013)

Sekerbayeva et al. (2020) performed an oil displacement test on a carbonate sample to check the effect of LSSF, as shown in Figure 15. An engineered water brine, made by 10 times dilution of seawater with 3- and 6- times spiked calcium and sulfate ion, with 1 wt% anionic surfactant was used during the flood. As a result, 70% of the OOIP was produced after tertiary flooding. The incremental oil recovery by hybrid EOR was 10%. Promising results reported in this study indicated the prospects of the hybrid chemical EOR method.

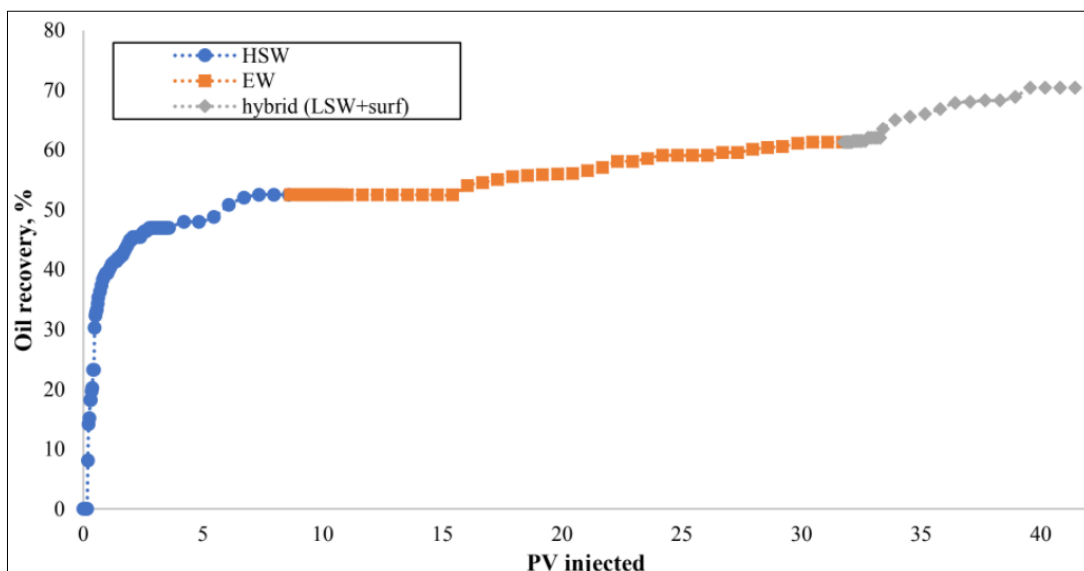


Figure 15. Oil recover (%) vs injected PV (Sekerbayeva et al., 2020)

Several experimental studies were done on the investigation of factors that influence the potential of hybrid EOR in sandstone (Khanamiri et al., 2016). The salinity and ions (Na^+ , Ca^{2+} ,

Mg²⁺) were adjusted during the study. Anionic surfactant and 10 times diluted seawater were used during the experiments. The experimental part of the work included the phase behavior, surfactant adsorption, and coreflooding test.

1.2.6 Negative salinity gradient

According to work done by Nelson (1982), the negative salinity gradient of the pre-flush water has a vital role in the establishment of an optimal salinity environment for surfactant flooding. Whenever surfactant concentration becomes lower due to retention and adsorption, the optimum salinity for surfactants starts to be unfavorable or too high for the lower amount of surfactant. That is why the salinity of pre-flush water is designed to be in descending order.

The optimal amount of injected PV and surfactant concentration was discussed in Todd et al. (1978) work (Sheng, 2011), where the effectiveness of flooding of large PV with a low concentration of surfactant and small slug with a high concentration of surfactant were compared. As a result, the second case showed more preferable results and higher oil recovery. Studies of Gogarty (1976) and Murtada and Marx (1982) have proved the validity of the previous conclusion that recovery characteristics for high concentration surfactant flooding are more efficient than low concentration. Moreover, a simulation study was done by Tavassoli et al. (2016) using UTCHEM-IPhreeqc. Flooding of LSW and surfactant was modelled and confirmed the results of the experimental study of Tahir et al. (2018). The purpose of the simulation was to prove the effect of a properly selected surfactant and flood design with the combination of LSW and other injection parameters of pre-flush brine on oil recovery. There is a knowledge gap on the effect of negative salinity gradient on the performance of surfactant flooding in carbonates. This design should be considered to achieve a more efficient hybrid EOR.

1.3 Problem definition

Analyzing the available literature reveals a deficiency of in-depth study on stand-alone LSWF, surfactant flooding and the hybrid LSSF EOR techniques in carbonate reservoirs. Hence, the focus of the current research is to study the performance of LSWF in combination with SF in carbonates. The objective is to suggest numerous hybrid flooding designs and to measure oil displacement efficiency and associated parameters, such as retention. Different coreflooding tests were designed to study the performance of the hybrid method and to investigate the effect of injection design scheme, such as negative salinity on the oil recovery.

There are a few studies done on surfactant adsorption on carbonates and negative salinity gradient design in carbonates. It is of interest to conduct relevant laboratory studies in this area. Alagic & Skauge (2010), Alagic et al. (2011), Khanamiri et al. (2015), Johannessen & Spildo (2016) investigated the effectiveness of synergy of low salinity waterflooding with low salinity surfactant flooding, but almost all oil displacement tests were conducted on sandstone core samples. Thus, it is important to conduct laboratory coreflood analysis in carbonates to further investigate this topic.

1.4. Objectives of the Thesis

1.4.1 Main Objectives

The following objectives should be achieved to analyze and identify the best hybrid CEOR design for carbonates.

- Analyze previous experimental studies done on hybrid CEOR evolving the work of low salinity water and surfactant;
- Select the optimal alkali (Na_2CO_3) concentration in terms of ultra-low IFT provision and effect on the adsorption of an anionic surfactant on the carbonate surface;
- Design and conduct coreflooding oil displacement tests;
- Identify the appropriate injection scheme, such as negative gradient procedure.

1.4.2 Thesis Structure

Chapter 2 provides information about the methodology of the research work, which is one of the key parts of the thesis. The methodology part explains the selected experimental methods.

This section describes the list of materials required to conduct laboratory analysis. It includes the information about utilized formation water, engineered water (EW), Caspian Sea water, crude oil, rock and chemicals. Moreover, chapter 2 represents the details and sequence of the procedures done to achieve thesis objectives. Solution preparation, basic rock and fluid property measurements, aqueous stability, phase behavior, static adsorption tests and step by step coreflooding experiment instructions explained.

Chapter 3 presents and analyzes the obtained experimental results. This section summarizes the most optimal alkali/surfactant formulation in terms of phase behavior, aqueous stability and static adsorption tests. Identified optimal injection fluids were used to design coreflooding experiments. This chapter examines the oil recovery of each coreflood design.

Chapter 4 summarizes the significant outcomes of the research work and provides suggestions about possible improvements..

2 Methodology

This chapter presents detailed information about the materials and methodology followed in the conducted experiments in this research. Understanding oil displacement by the hybrid chemical EOR technique, which involves mutual work of surfactant, alkali, and low salinity water, requires a comprehensive experimental study. Hence, different experiments were designed, conducted, and analyzed to achieve research objectives and answer questions raised in this area. The main purpose is to design several hybrid EOR coreflooding experiments to analyze the oil displacement performance and oil/brine/chemicals/LSW interactions during the EOR process. Previous research results (Sekerbayeva et. al., 2020) were used as a base of the hybrid EW/surfactant CEOR in this study. Experiments were conducted to show the effect of adding alkali (Na_2CO_3) to the CEOR slug on the adsorption of an anionic surfactant on the carbonate surface and the oil recovery. The injection sequence scheme was also analyzed to investigate the effect of a negative salinity gradient on the oil displacement and recovery during EW/surfactant CEOR.

First, aqueous stability and phase behavior tests were done to measure the properties and interactions of oil/brine/chemicals at the operational temperature. Basic rock and fluid property measurements were carried out to perform intermediate calculations and to check crude oil-brine-rock system compatibility. The following steps were followed to analyze the hybrid chemical EOR performance:

- Tailoring and designing the optimized EW after adding alkali (Na_2CO_3) to the surfactant solution to develop middle phase microemulsion at the reservoir temperature;
- Designing injection brine composition and sequence for CEOR at negative salinity gradient condition;
- Comparing static adsorption on carbonate rock surface for surfactant solutions and surfactant-alkali solutions;
- Performing coreflooding experiments to analyze the oil recovery and fluid flow for different CEOR designs.

2.1 Materials

This part of the methodology provides information about the materials utilized in this work. Reservoir rock/fluids such as formation brine, reservoir rock, and injection brine were used to study the hybrid method for the possible implementation in Kazakhstan's oil fields.

2.1.1. Core Samples

Oil displacement studies were performed on carbonate samples. 4 similar core samples were prepared from a limestone outcrop to perform core flooding experiments. Typically, the length of core samples was 73 mm, and the diameter was 38 mm, as depicted in Figure 16. Table 2 provides the basic properties of the core samples. The powder of the core sample was analyzed using XRD (X-ray diffraction) to determine the mineralogical composition. According to the XRD results, the rock samples consist of 99.97% calcite (CaCO₃) and 0.03% quartz (SiO₂).

Table 2. Core samples primary measurements

	Diameter, mm	Length, mm	Dry weight, g	Porosity, %	Absolute permeability, mD	Effective Permeability, mD	S _{wi}
Core-1	38.06	73.03	185.54	16.02	94.04	90.17	0.19
Core-2	38.08	73.11	185.93	15.43	83.60	79.54	0.13
Core-3	38.10	73.00	187.70	14.63	163.87	112.55	0.12
Core-4	38.10	73.06	186.81	14.47	117.09	111.54	0.12



Figure 16. Limestone core sample

2.1.2. Brine

Several brine samples were utilized to mimic the formation and different injection water types. Table 3 presents required salts to prepare brines. Primarily, the formation water was prepared based on the composition of the formation water in a field in West Kazakhstan. This brine was used to saturate core samples to establish the initial reservoir condition. Table 4 provides the composition of formation water, which has a total salinity of 181,980 ppm. The absolute permeability of cores was obtained by flooding with 100% formation water.

Table 3. Chemicals used for brines preparation

Required chemicals	Chemical formula	Purity	Producers
Sodium bicarbonate	NaHCO ₃	≥99.0%	SIGMA-ALDRICH
Sodium sulfate	Na ₂ SO ₄	≥99.0%	
Sodium chloride	NaCl	≥99.0%	
Calcium chloride dihydrate	CaCl ₂ .2H ₂ O	≥96.0%	ACROS ORGANICS
Magnesium chloride hexahydrate	MgCl ₂ .6H ₂ O	≥99.0%	SIGMA-ALDRICH

Table 4. Composition of major ions of formation water (Isabaev Y. et. al., 2015)

Ions	Formation water, ppm
Na ⁺ + K ⁺	81,600
Ca ²⁺	9540
Mg ²⁺	1470
Cl ⁻	90,370
Total	181,980

South Caspian Seawater from West Kazakhstan was selected as the base injection brine for core flooding experiments. Table 5 reveals the ionic composition of South Caspian Seawater, which has a total salinity of 13,000 ppm.

Table 5. Ionic composition of South Caspian Seawater (Tuzhilkin, et al., 2005)

Ions	South Caspian Sea (SW), ppm
Na ⁺ + K ⁺	3240
Ca ²⁺	350
Mg ²⁺	740
Cl ⁻	5440
SO ₄ ²⁻	3010
HCO ₃ ⁻	220
Total	13,000

According to previous work (Sekerbayeva et.al 2020), the most suitable engineered water is 10 times diluted Caspian Seawater with 3- and 6- times spiked calcium and sulfate ions respectively (10xSW-6SO₄, Mg, 3Ca). This brine affects the rock/oil/formation brine the most

and results in the highest alteration in wettability to the water-wet state. In this study, we used this optimized brine to be applied during the oil displacement tests by the hybrid method. Thus, the combination of the optimized engineered water with anionic surfactant was used to study the effect on the capillary number and oil recovery. Table 6 demonstrates the chemical composition of engineered water.

Table 6. Ionic composition of the optimized engineered water (EW)

Ions	Concentration of the optimized EW, ppm
$\text{Na}^+ + \text{K}^+$	325
Ca^{2+}	105
Mg^{2+}	74
Cl^-	544
SO_4^{2-}	1806
HCO_3^-	22
Total	2876

Two core flooding experiments were designed to study the effect of negative salinity gradient on the surfactant flooding performance. Primarily, this concept was suggested by Nelson and Pope (1978). The highest oil recovery was obtained during the coreflooding experiment, where salinities in the pre-flush water, chemical flood and post-flush water drive were in descending value. Surfactant concentration decreases during propagation through the core sample, because of the dilution and adsorption, thus optimal salinity is lowered (Glover et. al, 1979). Hence, the optimum salinity measured by phase behavior may change and be lowered in the porous media, leading to the modification of the salinity and generation of the Winsor Type III microemulsion in the porous media. Through application of the negative salinity gradient injection scheme, the salinity alters the optimum condition in the porous media to maintain the presence of the microemulsion phase as long as possible. Moreover, surfactant early breakthrough can be excluded during surfactant partition into the oil phase under an over-optimum salinity state (Hirasaki, 1981).

Following this line of investigation, we studied the effect of the negative salinity gradient scheme and compared it to normal surfactant flooding at the optimum salinity. Two negative salinity sequences were designed as shown in Figure 17 and Figure 18. Table 7 and Table 8 provide injection brine compositions for two negative salinity gradient flooding designs.

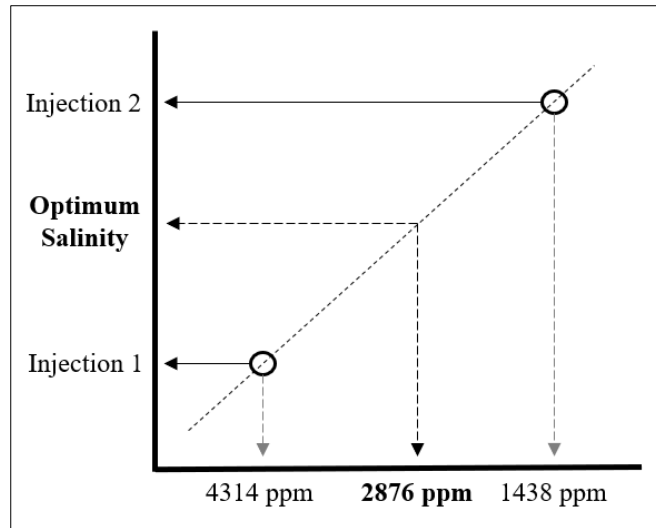


Figure 17. Schematic diagram of salinity design for core flooding experiment #3

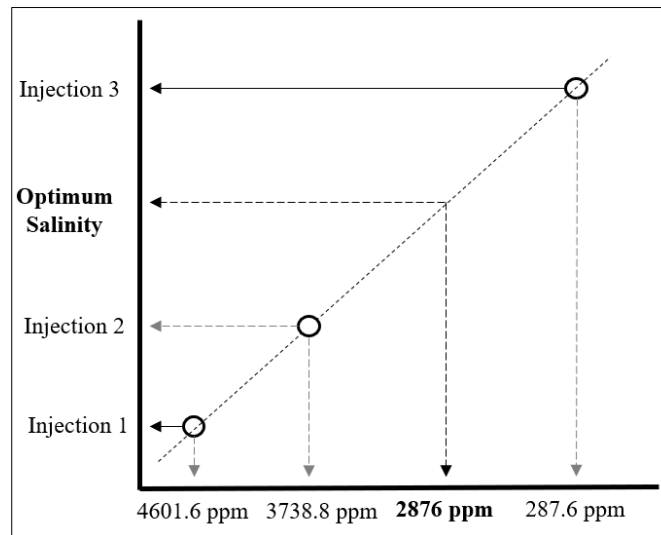


Figure 18. Schematic diagram of salinity design for core flooding experiment #4

Table 7. Injection brine composition for core flooding experiment #3

Ions	Optimum Engineered Water, ppm	Injection 1, ppm	Injection 2, ppm
Na ⁺ + K ⁺	325	487.5	162.5
Ca ²⁺	105	157.5	52.5
Mg ²⁺	74	111	37
Cl ⁻	544	816	272
SO ₄ ²⁻	1806	2709	903
HCO ₃ ⁻	22	33	11
Total	2876	4314	1438

Table 8. Injection brine composition for core flooding experiment #4

Ions	Optimum Engineered Water, ppm	Injection 1, ppm	Injection 2, ppm	Injection 3, ppm
Na ⁺ + K ⁺	325	520	422.5	32.5
Ca ²⁺	105	168	136.5	10.5
Mg ²⁺	74	118.4	96.2	7.4
Cl ⁻	544	870.4	707.2	54.4
SO ₄ ²⁻	1806	2889.6	2347.8	180.6
HCO ₃ ⁻	22	35.2	28.6	2.2
Total	2876	4601.6	3738.8	287.6

2.1.3. Crude oil

The crude oil that was used in this study was taken from a carbonate oil field in the Aktobe Region, West Kazakhstan. Table 9 reveals crude oil composition. The crude oil is medium-heavy in density (0.867-0.907 g/cm³), has low sulfur content (0.1-0.14%), is slightly paraffinic (0.52-2.06%), and has a high amount of resins (15-21.5%) (Marabayev et al., 1999). More detailed measurements, such as density and viscosities at different temperatures, are illustrated in Figure 19. Crude oil parameters were estimated with the assistance of a SVM 3001 Viscometer from Anton Paar equipment. The measured total acid number (TAN) of crude oil was 4.3 mg KOH/g. The AN value shows that this crude oil is suitable for alkali/surfactant and engineered water flooding.

Table 9. Crude oil composition

Component	C5	C6	C7	C8	C9	C10	C11	C12	C13	C14	C15+	other
wt%	0.8	0.43	1.63	7.36	8.7	17.87	5.09	5.44	8.3	6.15	30.55	7.66

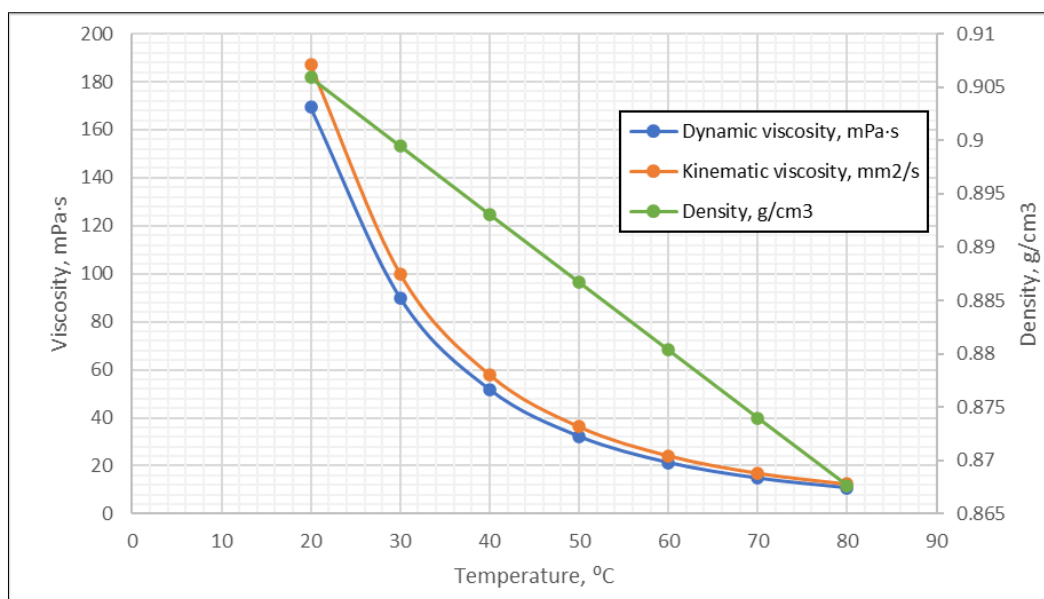


Figure 19. Crude oil dynamic, kinematic viscosity, and density versus temperature

2.1.4. Surfactant

Anionic surfactant, namely Soloterra-113H (benzenesulfonic acid, 4-C10-13-sec- alkyl deriv.), was used for phase behavior tests and core flooding experiments. It was provided by the Sasol company. According to prior studies (Sekerbayeva et.al 2020), Soloterra-113H in combination with the optimized engineered water (10xSW-6SO₄, Mg, 3Ca) provided the most effective microemulsion phase and low IFT between the oil and water phases. Moreover, the aqueous solution with Soloterra 113H showed the best stability at 20 °C and 80 °C. Anionic surfactants are cost-effective compared to cationic surfactants. Table 10 provides the information about Soloterra 113H surfactant.

Table 10. Anionic surfactant characteristics

Type of surfactant	Chemical Name	Physical state	pH	Boiling/Cond. Point (properties @25 ^o C)	Flash point	Chemical stability at normal cond.	Hazards identification GHS Classification
Surfactant/Sasol Activity: 96.5% w/w	Benzenesulfonic acid, 4-C10-13-sec- alkyl deriv.,	Brown viscous liquid	<2	density– 1.06g/cm ³ , viscosity dynamic– 2400 mPas	210 °C	Stable	Acute toxicity Category 4 Chronic aquatic toxicity Category 3

							Skin corrosion Category 1C
--	--	--	--	--	--	--	----------------------------------

2.1.5. Alkali

To control anionic surfactant adsorption on the carbonate surface and to study the effect of ASP on the oil recovery, an alkali (Na_2CO_3) was used. It was provided by SIGMA-ALDRICH company. The addition of alkali promotes ultralow IFT by surfactant generation in-situ while interacting with acids crude oil.

2.2 Procedures

This part of the methodology explains the work sequence, equipment, and how experiments were done.

2.2.1 Brine, surfactant, alkali solutions preparation

The fluid preparation process required weighing balance and a magnetic stirrer. Table 11 introduces the list of salts added to prepare brines. The magnetic stirrer was set to 800 rpm to provide constant mixing of distilled water with salts. Once EW was prepared, the anionic surfactant was added slowly with a constant mixing speed of 200-300 rpm to prevent foaming. The concentration of surfactant for coreflooding, aqueous stability, and phase behavior tests was 10,000 ppm.

Table 11. Mass of salts required to prepare different brines

Salts	Formation brine (FW), g/L	Caspian Sea Water (SW), g/L	Engineered water, g/L
NaCl	207.42	4.36	-
Na_2SO_4	-	4.45	1.34
$\text{CaCl}_2 \cdot 2\text{H}_2\text{O}$	34.98	1.28	0
$\text{MgCl}_2 \cdot 6\text{H}_2\text{O}$	12.28	6.18	0.31
KCl	1.32	-	0.19

As alkali addition to surfactant solution increases the ion content, several phase behavior tests were done to adjust the composition of the optimized engineered water. As a result, the engineered water was diluted 1.5 times to achieve the largest microemulsion phase. To make the alkali-surfactant solution, alkali (Na_2CO_3) was mixed with the distilled water and then

slowly added to the surfactant solution, which is prepared in the engineered water. Thus, in the end, it gives 1.5 times diluted Engineered water with alkali and surfactant. 5 different concentrations of alkali were used to perform solutions at concentration of 0.5%, 0.75%, 1%, 1.25%, and 1.5% of the aqueous phase.

2.2.2 Rock and fluid properties measurements

Crude oil was filtered from any impurities and then degassed using a magnetic stirrer to make it appropriate for viscosity and density measurements. The viscosity and density of crude oil were measured at different temperatures from 20 °C – 80 °C with the step of 10° C using an SVM 3001 Viscometer from Anton Paar, as shown in Figure 20.



Figure 20. SVM 3001 Viscometer

Similarly, formation water viscosity and density were recorded to perform further required calculations. Also, crude oil total acid number (TAN) was identified by the titration technique described in ASTM standard test procedure (D974). The titration solvent was prepared by mixing 500 ml of toluene, 495 ml of isopropanol and 5 ml of distilled water. As a titrant 0.1N KOH solution prepared in isopropanol was used. First, a blank titration was conducted by using 100 ml of solvent and adding 0.05 ml of phenol phthalein indicator solution to solvent. The uniform solution was achieved by stirring 30 seconds. Then titrant was added drop by drop with a 1 ml syringe until the solution turned to pink color. The volume of titrant consumed was noted. Similarly, the titration was performed with the crude oil sample. 1g of oil was weighed in titration flask and mixed with 100 ml of solvent until the total oil dissolution. 0.05 ml of indicator solution was added to mixture and mixed for 30 seconds. The sample was then titrated with KOH solution until the solution changed color from brown to pink. The volume of titrant consumed was noted and AN was determined using Equation 2.2.2.a:

$$TAN = \frac{\text{Volume of titrant (ml)} * \text{Normality of KOH} * 56.1}{\text{Mass of sample (g)}} \quad (2.2.2. a)$$

The basic properties of core samples were measured. Length and diameter measurements were taken using a caliper to determine the bulk volume of the core samples. The cores samples were also left in the oven at 60°C for 24 hours before weighing until they were completely dry. After determining the dry weight of the core samples, the porosity was measured using a Helium Porosimeter by Vinci-Technologies. To restore initial conditions of core samples and to cross-check the porosity, core samples were placed in a Manual Saturator by Vinci-Technologies as Figure 21 presents. The core samples were evacuated by a vacuum pump for 1 h, then saturated with formation water at 1200 psi pressure for 4-6 hours until pressure stabilization. Saturated core samples were then inserted into formation water with a salinity of 181,980 ppm for 3 days. Saturated core samples were weighted, and the porosity was estimated by Equation 2.2.2.b:

$$\varphi = \frac{\frac{m_{\text{saturated}} - m_{\text{dry}}}{\rho}}{\pi \left(\frac{d}{2}\right)^2 L} \quad (2.2.2. b)$$

$m_{\text{saturated}}$ – sample weight fully saturated, g

m_{dry} – sample weight clean and dry, g

ρ – density of saturation liquid, g/cm³

d – sample diameter, cm

L – sample length, cm



Figure 21. Manual Saturator (AP-007-001-1) by Vinci-Technologies

To mimic the initial conditions of core samples and to measure the absolute permeability by brine, the core samples were flooded with the formation water using the Aging Cell Apparatus by Vinci-Technologies which is shown in Figure 22. To attain reservoir conditions, the heating mantle temperature was set at 80° C, the unit confining pressure was regulated between 1000-1200 psi, and the backpressure was settled at 500 psi. Pressure data were recorded for each pore volume at 3, 5, 7, 9, 12 cc/min flow rates. Recorded results were used to estimate the absolute permeability of each core sample using Darcy’s equation. Filtered crude oil was injected into the core sample to measure the effective permeability by oil. After the injection test, the core samples were inserted into an aging cell filled with the oil, which was placed in the oven at 80°C for several days to alter the wettability of the core sample toward the oil-wet state as Table 2.2.2 presents.

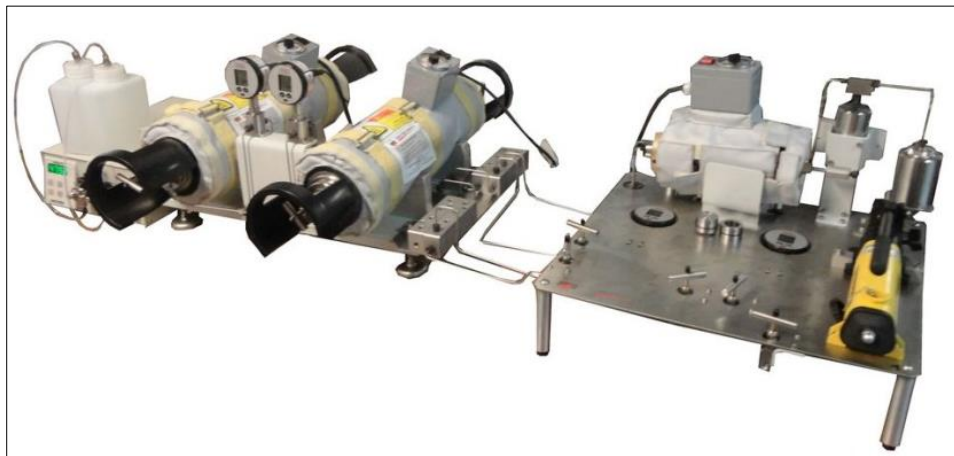


Figure 22. Aging Cell Apparatus (ACA 700)

2.2.3 Aqueous stability and phase behavior tests

Theoretically, the cationic surfactants are functional in carbonates due to electrostatic repulsion, which causes low adsorption on the rock surface. Furthermore, the reason for the broad utility of cationic surfactants in carbonates is wettability alteration from oil-wet to more water-wet behavior and reduction in loss of surfactant (Mwangi, 2010). However, some studies showed a comparatively equal adsorption level of anionic and cationic surfactants (Rosen and Li, 2001; Ma et al., 2013). The alkali addition (Na_2CO_3) can reduce IFT and lower static adsorption of surfactant by altering the surface charge of carbonate to a negative value. Hence, the point of these tests was to analyze the phase behavior, to determine the aqueous stability of an applicable anionic surfactant, and to study the effect of alkali addition. Anionic surfactants are more efficient in attaining an ultralow IFT between two phases and are moderately inexpensive (Kamal et. al, 2017). Hence, in our study, we want to show the possibility of

improvement of the performance in oil recovery of anionic surfactant and reduction of the operational problems, such as retention, by using low salinity alkali/surfactant formulation in a hybrid EOR method.

Alkali influences the phase behavior of anionic surfactant systems, because they provide a supplementary source of cationic electrolyte (Martin and Oxley, 1985). The salinity of the water has a significant impact on the phase behavior of the surfactant solution. The water solubility of anionic surfactant becomes lower when the salinity of formation water increases. Surfactants start to move from the water phase to the oil phase as the electrolyte concentration progressively increases. Hence, when the salinity of brine increases, the surfactants migrate to the oleic phase from the aqueous phase, i.e. from Winsor Type I to Type II through Type III. Figure 23 illustrates a schematic representation of the phase behavior tests. When the aqueous phase salinity becomes higher, the solubility of anionic surfactants in the aqueous phase decreases, thus surfactants are driven out of the brine and contribute to the middle or upper phase and cause the transition of microemulsion from Type I to Type II through Type III.

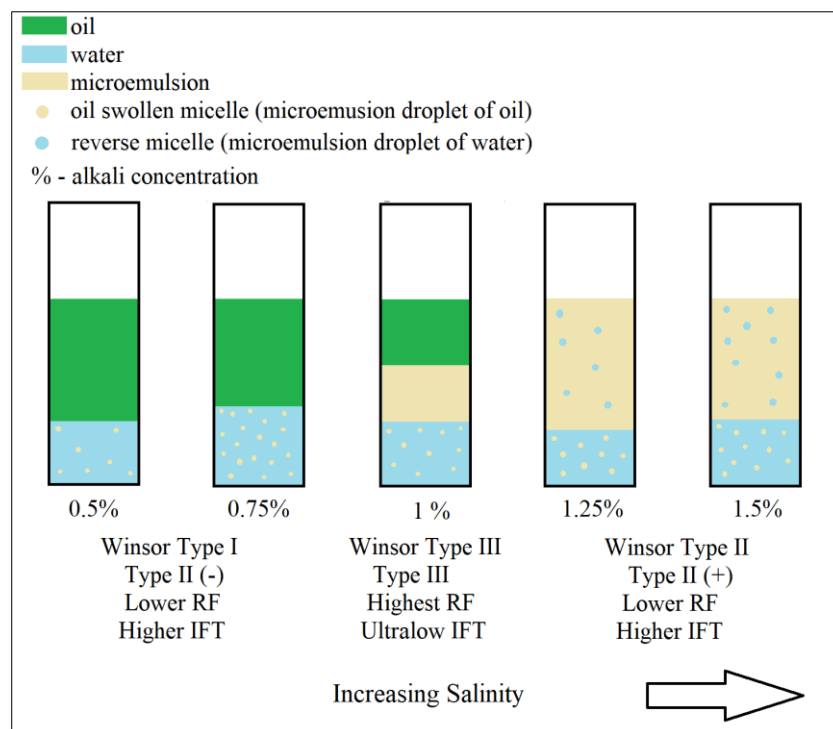


Figure 23. Schematic illustration of middle phase formation and microemulsion phase transition as a function of salinity

An increase in alkali concentration leads to a reduction in optimal salinity. That is why the selected engineered water is no longer optimal as a surfactant solution once alkali is introduced. To investigate the potential of a more economical blend, i.e., a lower concentration of alkali

and surfactant, the screened concentration of Na_2CO_3 was varied from 0.25% to 1.5% in the aqueous solution. The phase behavior is a significant test to select the proper type and the concentration of surfactant or alkali. Figure 23 shows the phase behavior of oil, brine, and surfactant/alkali. This figure supports that the addition of alkali to the surfactant solution shifts the phase behavior and vanishes the microemulsion phase. Hence, new phase behavior analyses are required to tailor the engineered water design that provides the highest solubilization ratio and an effective microemulsion phase.

An equal volume of crude oil (2 mL) and solution (2 mL) were mixed in a 10 mL vial. Different solutions were prepared by mixing Soloterra 113H surfactant in the concentration of 1 wt% with the engineered water, and the alkali (Na_2CO_3) with the concentration of 0.25%, 0.5%, 1%, and 2% of the aqueous phase. The samples were gently agitated on vials with a mixing angle of 30° for 15 minutes. Half of the solutions were ready to stand in the oven at 80°C for 6 days before the phase behavior study. The other half of the vials were also left at 25°C for 6 days.

The aqueous stability test is required to examine the compatibility of surfactants with the low salinity water and other chemicals. According to the previous work of Sekerbayeva et.al (2020), the solution consisting of Soloterra 113H surfactant and engineered water (10xSW-6 SO_4 , Mg, 3Ca) demonstrated stable behavior at reservoir (80°C) and room (25°C) temperatures. Similar aqueous stability tests were conducted to study the effect of alkali on the surfactant solution stability mixing with 1.5 times diluted engineered water. Samples were prepared with 1 wt% surfactant concentration, and different concentrations of alkali (Na_2CO_3) as 0.5%, 0.75%, 1%, 1.25% and 1.5% of the aqueous phase. Two sets of solutions were prepared and poured into 10 mL vials. A portion of the vials were placed in the oven at 80°C and companion vials were left at 25°C . After 6 days, the samples were analyzed for clarity and absence of precipitation.

2.2.4 Static adsorption test

The retardation of the surfactant front caused by adsorption onto the formation rock leads to an inefficient and economically challenging oil recovery process. Therefore, the adsorption behavior of a surfactant needs to be systematically investigated before its application in CEOR and our proposed hybrid method.

Five (5) surfactant solution samples with concentrations of 0.6 wt%, 0.8 wt%, 1 wt%, 1.2 wt%, and 1.4 wt% of Soloterra 113H were prepared and tested through the UV-Vis

Spectrophotometer as shown in Figure 24. EW was used as a baseline for the surfactant static adsorption test. Then the calibration curve for surfactant adsorption was plotted.



Figure 24. Evolution 300 UV-Vis Spectrophotometer

After that, surfactant solution with Soloterra 113H of 1wt% concentration, and 5 samples with alkali (Na_2CO_3) concentration of 0.5%, 0.75%, 1%, 1.25% and 1.5% of the aqueous phase were prepared. 50 nm-sized limestone powder was obtained by crushing the limestone core samples to check and compare the static adsorption of surfactant and alkali by rock surface. The limestone powder was cleaned up by distilled water and dried at 80°C in the oven for 24 hours as shown in Figure 25. Then, the powder was mixed with the surfactant and alkali/surfactant samples in a ratio of 2:1. The mixtures were inserted into aging cells and placed in a roller oven to provide proper mixing for 5 days.



Figure 25. Roller oven

The adsorption process was qualified following several days of mixing as follows. 10 mL of solution samples were taken from the aging cells. 2 days were allotted for the powder to settle in the solution. Those samples were tested through the UV-Vis Spectrophotometer. Surfactant

concentration after the static adsorption test was calculated with help of an equation taken from the calibration curve. Then adsorption density was calculated by Equation 2.2.1:

$$q = \frac{V(C_0 - C_e)}{G} \quad 2.2.1$$

where q represents the adsorption density (mg/g); C_0 is the initial surfactant concentration (mg/L); C_e is the surfactant concentration after the static adsorption by rock (mg/L); V is the volume of surfactant and alkali/surfactant solution (L); G is the powder weight (g).

Calculated adsorption values of alkali/surfactant solutions were compared with the adsorption of surfactant concentration without alkali. In the end, the best alkali concentration in terms of static adsorption of surfactant was identified.

2.2.5 Coreflooding design

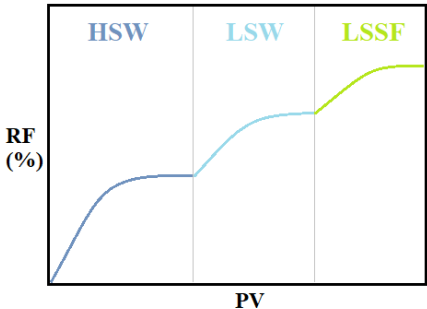
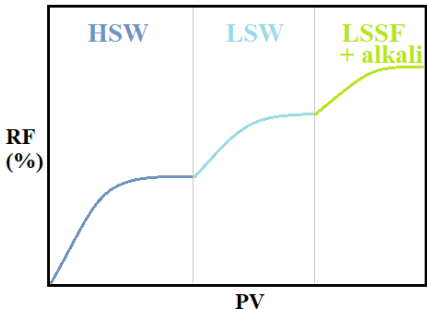
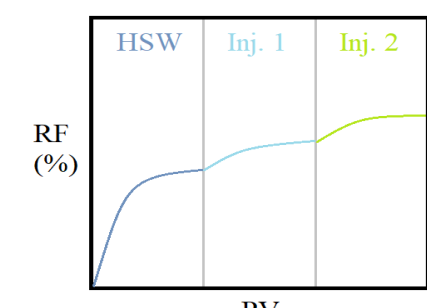
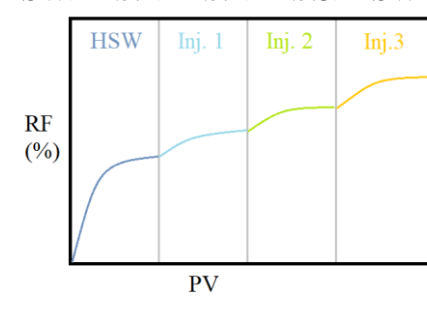
Based on the phase behavior test, the optimal surfactant-alkali concentration and EW salinity were screened. After the selection and testing of the injection fluids, five coreflooding experiments were designed. Those oil displacement tests are going to provide information about the efficiency of hybrid CEOR. The coreflooding experiment enables the analysis of oil recovery by different flooding designs, the effect of alkali addition, and negative salinity gradient.

The first core flooding experiment is designed to check the effect of low-salinity surfactant flooding and to confirm the results obtained by Sekerbayeva et. al (2020). It consists of three stages as shown in Table 12. As a pre-flush (or high salinity water) the Caspian Seawater was chosen. Then EW followed by the EW-surfactant solution was injected. The last step is post-flush water (EW) to ensure that there is no more oil production.

The second coreflooding experiment includes high salinity water (CSW) injection followed by EW and then optimized EW surfactant solution with the alkali (Na_2CO_3). This test was designed to test if the alkali can contribute to the oil recovery and how much.

The third and fourth experiments were designed to check the negative salinity gradient effect and to compare it with the previous tests. The difference between the third and fourth tests is the degree of the gradient. Details of the salinity of injection fluids can be found in Table 7 and Table 8.

Table 12. Coreflooding proposed designs

	Injection design	Injection fluid details
1. Hybrid Low Salinity Water (LSW) and Low Salinity Surfactant Flooding (LSSF)	<p>HSW>LSW>LSSF</p> 	<p>HSW – Caspian Seawater; LSW – Engineered water; LSSF – Engineered water with a surfactant of 10000 ppm concentration. Post-flush – Engineered water</p>
2. Hybrid Low Salinity Water (LSW) and Low Salinity Alkaline/Surfactant Flooding	<p>HSW>LSW>LSSF+Alkali</p> 	<p>HSW – Caspian Seawater; LSW – Engineered water; LSSF – EW with surfactant and alkaline at the optimized condition Post-flush – Engineered water</p>
3. Hybrid Low Salinity Water (LSW) and Low Salinity Surfactant Flooding (Negative Salinity Gradient)	<p>HSW>INJ.1>INJ.2>LSW</p> 	<p>HSW – Caspian Seawater; INJ.1 – Inj.1 with a surfactant of 10000 ppm concentration INJ.2 – Inj.2 with a surfactant of 10000 ppm concentration Post-flush – Engineered water</p>
4. Hybrid Low Salinity Water (LSW) and Low Salinity Surfactant Flooding (Negative Salinity Gradient)	<p>HSW>INJ.1>INJ.2>INJ.3>LSW</p> 	<p>HSW – Caspian Seawater; INJ.1 – Inj.1 with a surfactant of 10000 ppm concentration INJ.2 – Inj.2 with a surfactant of 10000 ppm concentration INJ.3. – Inj.3 with a surfactant of 10000 ppm concentration Post-flush – Engineered water</p>

2.2.5. Coreflooding

The final stage of the experimental part is the coreflooding oil displacement test. Injection fluids, oil-wet aged core samples, and coreflooding apparatus are required to fulfill the flooding objectives. Cut core samples were dried in the oven to characterize their basic properties:

porosity, permeability, dry weight, length, diameter, and total pore volume. After that, core samples were evacuated vacuumed and saturated with the formation brine. Once absolute permeability to brine and effective permeability to oil were measured, core samples were placed into the aging cell and filled with the crude oil.

The accumulators were filled with the injection fluids, and the system temperature was set at 80°C. Aged core samples were loaded into the coreholder and about 1200-1500 psi of confining pressure was applied. Also, the backpressure was set at approximately 500 psi. After the required installation, 1 hour was given to the system to reach 80°C and to stabilize the system pressure. All 4 core flooding experiments were conducted at a reservoir temperature of 80°C.

Before starting the injection of high salinity water, the core was flooded with oil rates of 0.5 cc/min, 2 cc/min, and then 5 cc/min to make sure that there is no movable water and S_{wi} is reached. All designed coreflooding experiments were started from high salinity water injection at the rate of 0.5 cc/min, 2 cc/min and 5 cc/min (0.2757 cm/min, 1.1027 cm/min, 2.7569 cm/min) until zero oil production, i.e., residual oil to waterflood. The next injection fluids followed the same procedure. In the end, the engineered water was injected to check that there is no more oil production. The produced effluent was collected into tubes, the produced oil volume and differential pressure for each pore volume were measured and noted in the excel sheet.

3 Results

This chapter presents the obtained results of experiments discussed in the methodology part of the research work. Experiments were conducted to identify alkali concentration and to design hybrid CEOR coreflooding tests. The results obtained from phase behavior and aqueous stability tests helped to adjust EW and alkali concentration to provide a middle phase microemulsion for better oil recovery and low IFT value.

The static adsorption experiment was done to demonstrate the positive effect of alkali addition on surfactant adsorption. As a result, the best alkali concentration was identified that provides the lowest adsorption of surfactant on the limestone surface.

The optimized alkali/surfactant formulation was used to design 4 core flooding oil displacement tests. There are hybrid low salinity-surfactant flooding, low salinity-alkali/surfactant flooding, and two negative salinity gradient experiments. This section analyzes the oil recovery of each core flooding test and determines the best hybrid CEOR design.

3.1 Screening of Alkaline/Surfactant solution

In the first stage, the effect of adding alkaline on the formation of phases in the oil/brine/surfactant mixture was studied. As Figure 26 shows, alkali concentration with 0.25% and 0.5% of aqueous phase gives Winsor Type I (Type II-) microemulsion, and 1%, 2% gives Winsor Type II (Type II+) microemulsion, which is not appropriate. Adding alkali increases the ions concentration which reduces the solubility of surfactant in brine and switches the mixture from Type II- to II+.

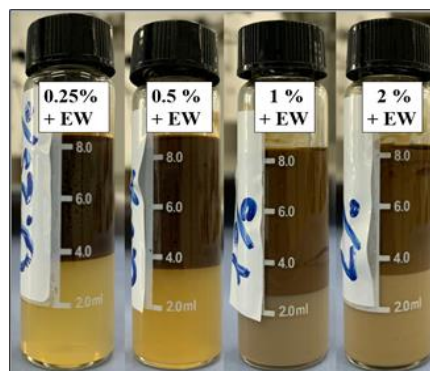


Figure 26. Phase behavior test at 80 °C for Na_2CO_3 concentrations of 0.25%, 0.5%, 1% and 2%



Figure 27. Phase behavior test at 80 °C for Na_2CO_3 concentrations of 1% of the aqueous phase with 1.5, 2, 4, 6 times diluted EW

To adjust the ions concentration, we decreased the brine salinity at 1% alkali concentration. Figure 27 demonstrates phases arrangement at different brine salinities. It is clear that at EW the mixture is Type II+, and at 4 times and 6 times diluted brines, it is type II-. Type III was achieved at 1.5 times dilution cases. Hence, it was decided to dilute EW for 1.5 times to achieve the best phase behavior. According to Figure 27, the alkali with the concentration of about 1% of the aqueous phase in combination with a surfactant solution prepared on 1.5 times diluted EW provides middle phase microemulsion or Winsor Type III (Type III). Table 12 reveals excess oil, water and microemulsion volumes.

Table 13. Phase volumes at 80 °C for Na_2CO_3 concentration of 1% of the aqueous phase with 1.5, 2, 4, 6 times diluted EW

Phase volume	EW	1.5*EW	2*EW	4*EW	6*EW
Oil, mL	0	2	4	4	4
Microemulsion, mL	5	3.5	0.1	0	0
Water, mL	3	2.5	3.9	4	4
Microemulsion type	II+	III	II-	II-	II-

To study the effect of temperature, phase behavior of the 1.5 times diluted EW with different concentrations of alkali was studied. Figure 28 and Figure 29 illustrate phase behavior tests done at 25 °C and 80 °C with different alkali concentrations. The favorable Type III or middle phase microemulsion can be found from the 1% of Na_2CO_3 case.

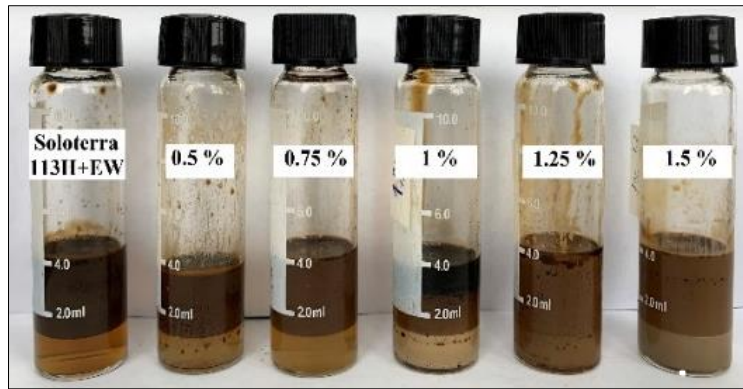


Figure 28. Phase behavior test at 25 °C for Na_2CO_3 concentrations of 0.5%, 0.75%, 1%, 1.25%, 1.5% with 1.5 times diluted EW

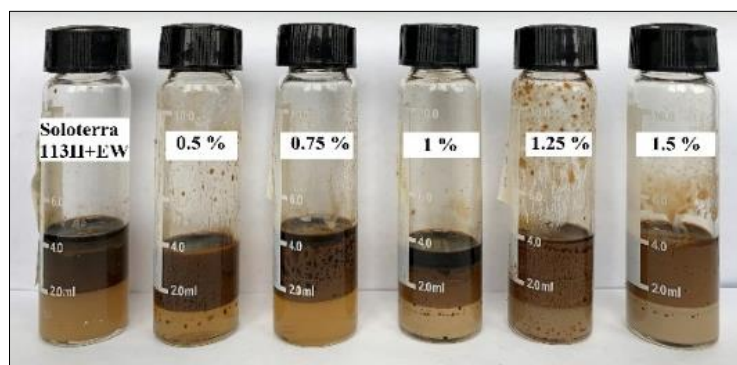


Figure 29. Phase behavior test at 80 °C for Na_2CO_3 concentrations of 0.5%, 0.75%, 1%, 1.25%, 1.5% with 1.5 times diluted EW

Figure 30 shows the plot of oil and water solubilization as a function of Na_2CO_3 concentration. It demonstrates that when alkali concentration is 0.5%, 0.75%, the water solubilization ratio is high and constant because all the water is solubilized in the microemulsion, whereas the solubilization ratio of oil is low. When the salinity increases, the solubilization ratio of oil also increases, while the solubilization ratio of water decreases. The intersection point of oil and water solubilization ratio curves versus salinity is the optimal salinity and optimal solubilization ratio.

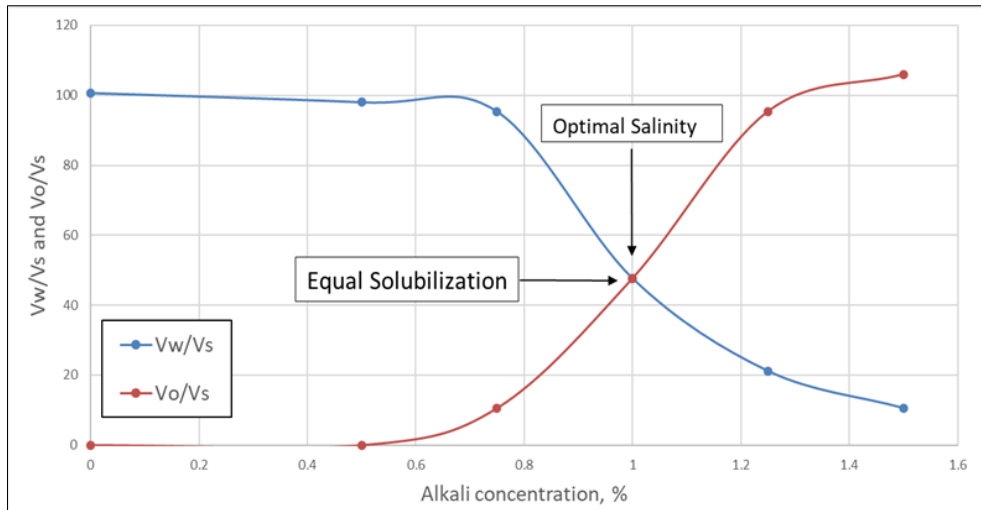


Figure 30. Microemulsion ratio of each sample

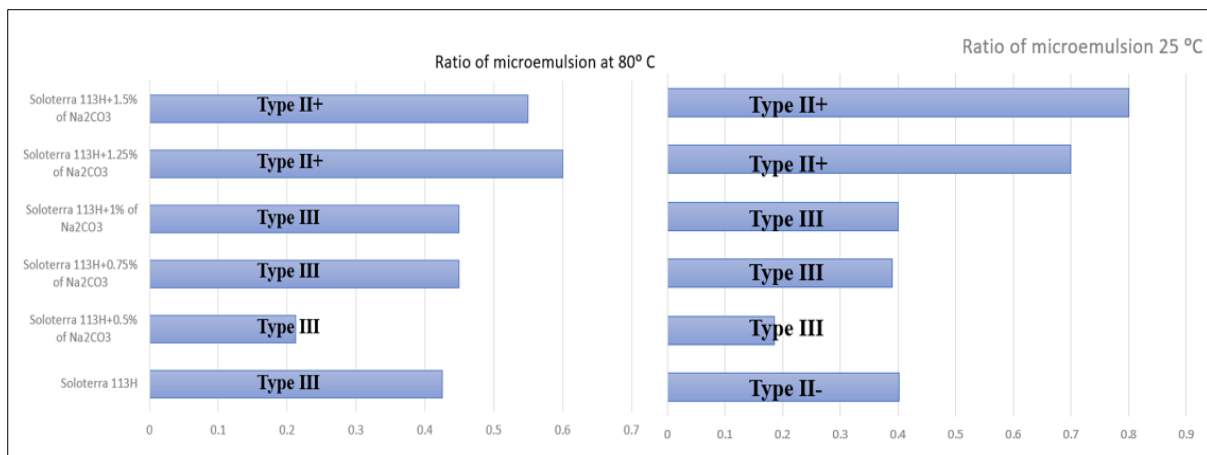


Figure 31. Microemulsion ratio of each sample

The aqueous stability test is required to examine the compatibility of surfactants with the low salinity water and other chemicals. According to the previous work done by Sekerbayeva et.al (2020), the solution consists of Soloterra 113H surfactant and engineered water (10xSW-6SO₄, Mg, 3Ca) demonstrated a stable behavior at the reservoir (80 °C) and room temperature (25 °C). Similar aqueous stability tests were conducted to study the effect of alkali on the surfactant solution stability mixing with 1.5 times diluted engineered water. Samples were prepared with 1 wt% surfactant concentration, and different concentrations of alkali (Na₂CO₃) as 0.5%, 0.75%, 1%, 1.25% and 1.5% of the aqueous phase. Two sets of solutions were prepared and poured into 10 mL vials. One part of the vials were placed in the oven at 80 °C and the other part of the same solutions were left at 25 °C. After 6 days the samples were analyzed for clarity and absence of precipitation. Figure 32 and Figure 33 represents the clarity of solutions at both temperatures. The first 4 samples demonstrate stable performance at both temperatures.

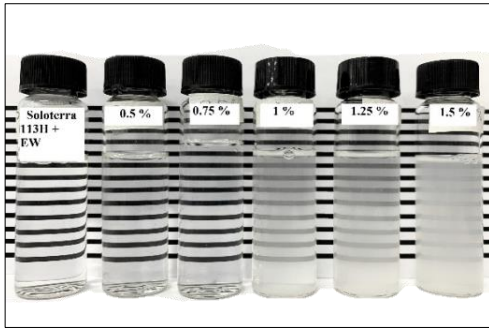


Figure 32. Aqueous stability test at 25 °C

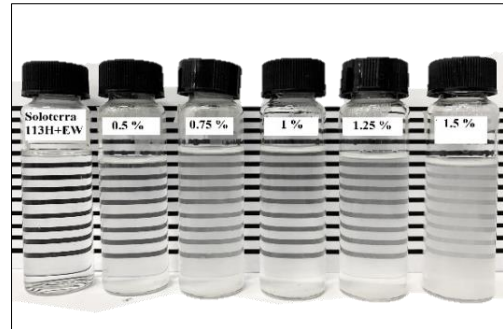


Figure 33. Aqueous stability test at 80 °C

3.2 Static adsorption test

First of all, the surfactant adsorption wavelength has to be selected to plot the calibration curve. Figure 34 presents a surfactant adsorption peak at 219 nm. Thus, the adsorption value for each surfactant concentration was used for the calibration curve construction as shown in Figure 35. The main theory for quantifying the adsorption density (mg/g) on the carbonate surface is to define the difference in surfactant concentration before and after adsorption.

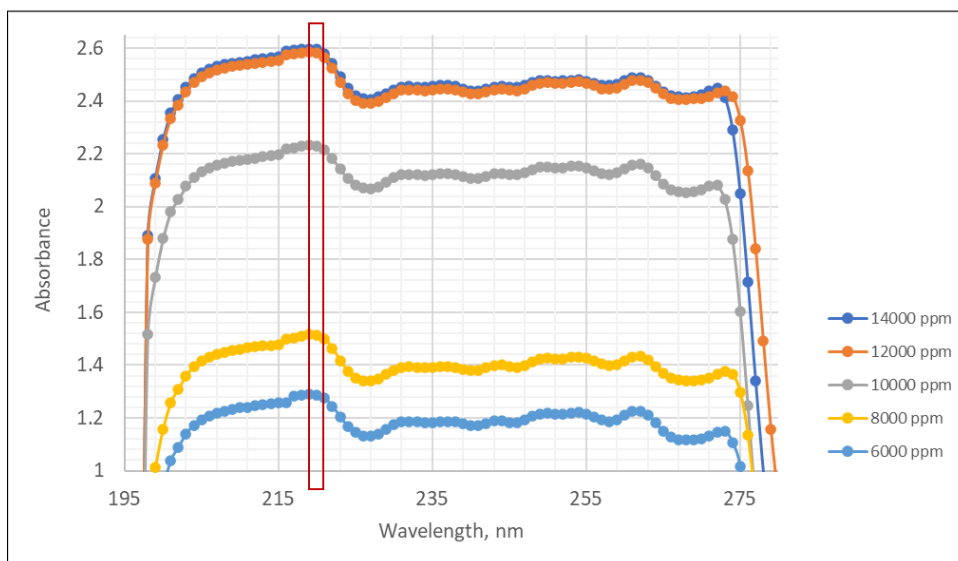


Figure 34. UV absorbance for each surfactant concentration

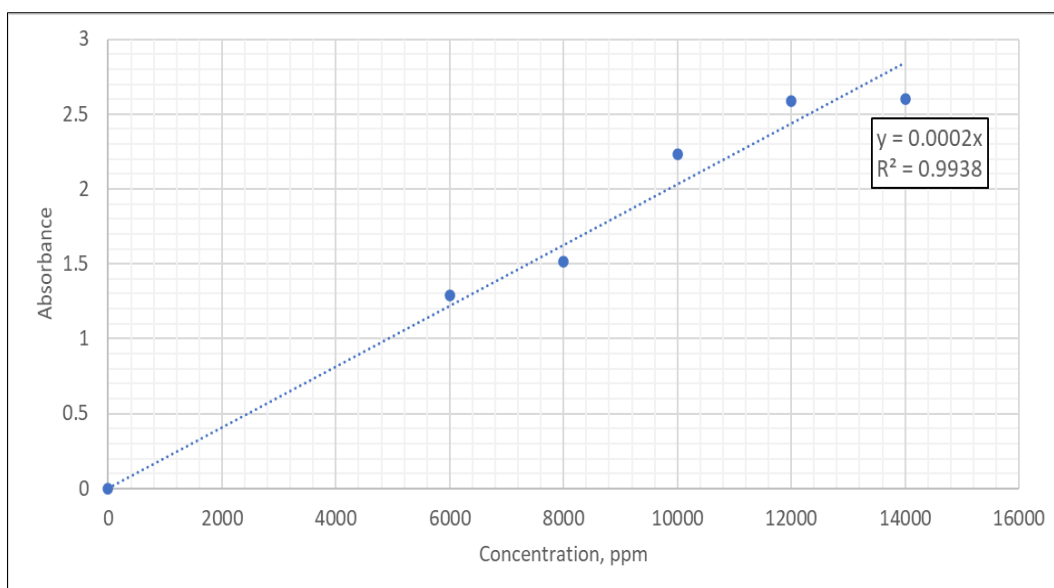


Figure 35. Calibration curve

Table 14. Calibration curve values

Concentration	0	6000	8000	10000	12000	14000
Absorbance at 219nm	0	1.289	1.515	2.232	2.585	2.598
Calibrated absorbance at 219 nm	0	1.254	1.654	2.054	2.454	2.854

Table 14 reveals the calibration curve values, calibrated absorbance shows the corresponding absorbance for each concentration in the ideal case. The equation of the trend line from Figure 35 was used to calculate the concentration of surfactant after mixing those solutions with the rock. Selected adsorption wavelength was used to note adsorption value after mixing the surfactant and alkali/surfactant solution with the limestone powder. Table 15 provides calculated adsorption density (q , mg/g) and remaining surfactant concentration (C_e). According to Table 15, the surfactant solution with the initial concentration of 10000 ppm shows 9475 ppm after mixing with the rock. 525 ppm of surfactant was adsorbed by the rock and the adsorption is 1.0194 mg/L. The purpose of introducing the alkali into the surfactant solution was to check to what extent the alkali will lower the surfactant adsorption.

Table 15. Adsorption density

Sample	C_e , mg/L	q , mg/g
Surfactant 10000 ppm	9475	1.0194
Surfactant 10000 ppm + alkali 0.50%	9590	0.7885
Surfactant 10000 ppm + alkali 0.75%	9720	0.5306
Surfactant 10000 ppm + alkali 1.00 %	9925	0.1473
Surfactant 10000 ppm + alkali 1.25%	10000	3.5044E-15

Surfactant 10000 ppm + alkali 1.50%	10000	3.5010E-15
-------------------------------------	-------	------------

Figure 36 presents the decrease in surfactant adsorption with the increasing alkali concentration. Alkali/surfactant solutions with an alkali concentration of 1.25% and 1.5% totally avoid surfactant adsorption. However, phase behavior and aqueous stability tests show that the alkali/surfactant solution with a concentration of 1% provides better results. In a static adsorption test, this alkali/surfactant formulation reduces the surfactant adsorption for 85.55% which has 0.1473 mg/g adsorption density.

Based on the above screening tests, 1% alkali concentration was selected as the optimum value to control surfactant adsorption, develop the microemulsion phase, and reduce the oil/brine IFT. To study the effect of the selected alkaline/surfactant/LSW hybrid combination on the oil recovery, coreflooding tests were conducted and analyzed.

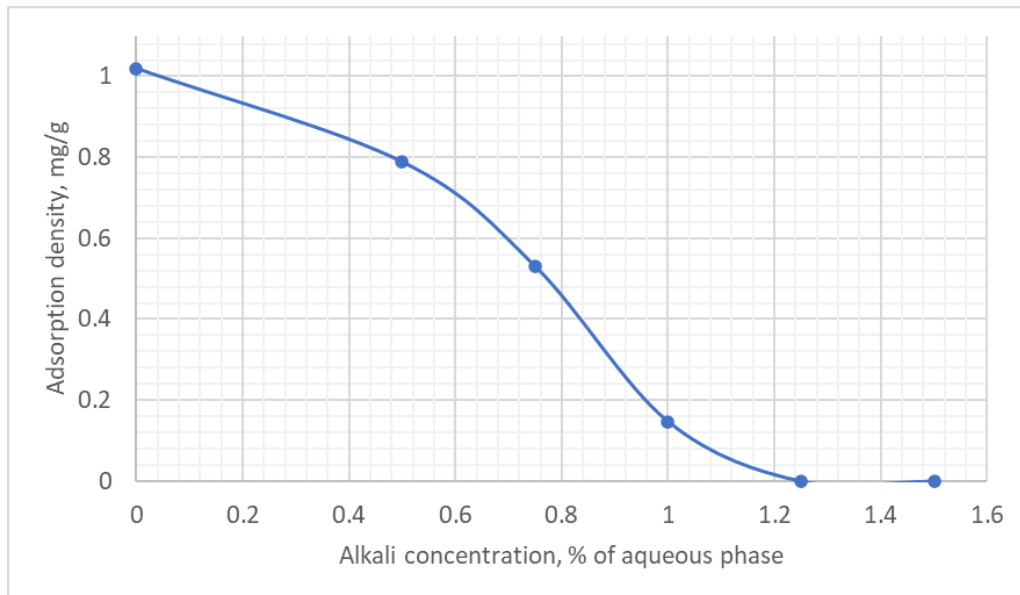


Figure 36. Adsorption vs alkali concentration

3.3 Coreflooding tests

Table 16 provides coreflooding experiment design details such as injection sequence, fluid type, concentrations of alkali and surfactant, injection rate.

Table 16. Coreflooding experiment details

Experiment №	Injection Fluid	Concentration	Injection Rate (cc/min)
1	HSW	-	0.5, 2, 5
	EW	-	0.5, 2, 5
	EWS	Surfactant: 1 wt%	0.5, 2, 5
	EW-Postflush	-	2, 5
2	HSW	-	0.5, 2, 5

	EW	-	0.5, 2, 5
	EWAS	1.5 times diluted EW Surfactant: 1 wt% Alkali: 1 wt% of the aqueous solution	0.5, 2, 5
	EW-Postflush	-	2, 5
3	HSW	-	0.5, 2, 5
	INJ. 1	Surfactant: 1 wt%-	0.5, 2, 5
	INJ. 2	Surfactant: 1 wt%	0.5, 2, 5
	EW-Postflush	-	2, 5
4	HSW	-	0.5, 2, 5
	EW	-	0.5, 2, 5
	INJ. 1	Surfactant: 1 wt%	0.5, 2, 5
	INJ. 2	Surfactant: 1 wt%	0.5, 2, 5
	INJ. 3	Surfactant: 1 wt%	0.5, 2, 5
	EW-Postflush	-	2, 5

The first oil displacement test was performed to check the effect of surfactant flooding in combination with EW on oil recovery. Surfactant flooding has the potential to significantly increase recovery over that of conventional waterflooding. The core sample used in this test has S_{wi} of 0.2 and a pore volume of 13.3 mL. HSW recovered 65.40%, EW recovered an additional 6.08% of oil in place. The total recovery before chemical flooding was 71.49%. Surfactant flooding recovered 11.04% of the total oil, which is 38.71% of residual oil. To sum up, this design recovered 82.53% of oil production. Figure 37 provides differential pressure and oil recovery data versus PV injected.

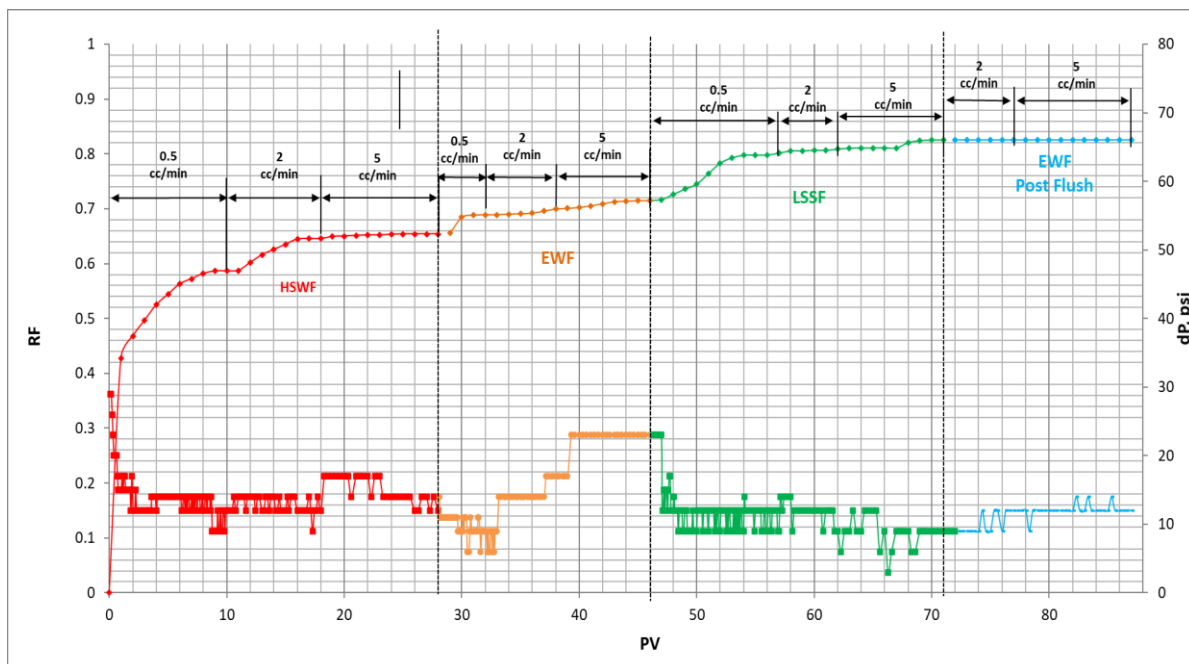


Figure 37. EWSF experiment results (dP and oil recovery vs PV injected)

In the next coreflooding experiment, surfactant/alkali was used in the CEOR stage. Compared to the previous EWSF test, the overall oil recovery was lower, which was 81.01%. HSW recovered 60.91% of oil, and EW recovered an additional 8.27% of oil. Before alkali-surfactant flooding, 69.17% of the oil was produced. Alkali-surfactant solution recovered 11.84% of incremental oil, which is 38.41% of the residual oil as shown in Figure 38.

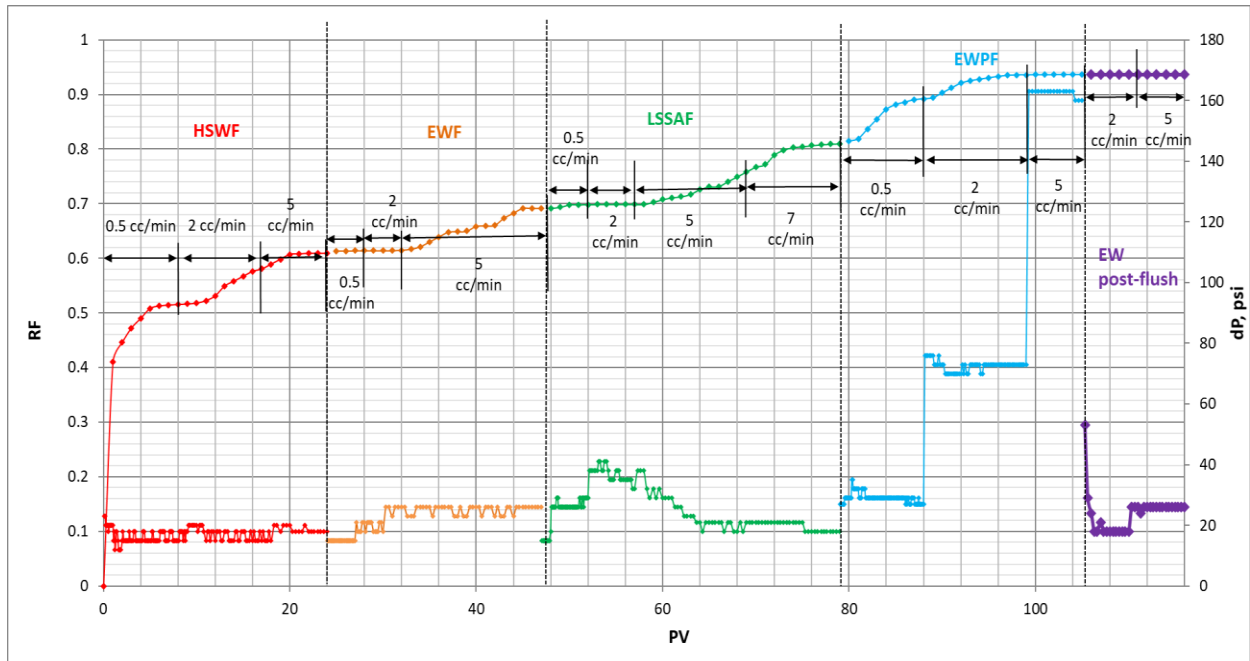


Figure 38. EWSF experiment results (dP and oil recovery vs PV injected)

Table 17. RF for EWSF and EWASF experiment results

Process	EWSF			Process	EWASF		
	RF (%OOIC)	Inc. RF	RF (%ROIC)		RF (%OOIC)	Inc.RF	RF (%ROIC)
HSW	65.40		65.40	HSW	60.91		60.91
EW	71.49	6.08	17.59	EW	69.17	8.27	21.14
EWSF	82.53	11.04	38.71	EWASF	81.01	11.84	38.41
	Total	17.12	-		Total	20.11	

Figure 39 represents the better effect of EWASF compared to EWSF in terms of ROIC for the CEOR part. EW and surfactant synergy gives 49.49% of ROIC and EW alkali/surfactant provides 51.43% of ROIC. EWASF flooding design demonstrates better performance compared to EWSF, resulting 20.11% of incremental oil recovery. This can be explained by

the significant IFT reduction with addition of alkali. IFT values were calculated by examining the phase behavior test and with help of Equation:

$$\log_{10}\sigma_{mo,mw} = \frac{4.80}{1 + 0.10(V_{0,w}/V_s)} - 5.40$$

The IFT value for EWSF was 0.02 dynes/cm and for EWASF was 0.000027 dynes/cm.

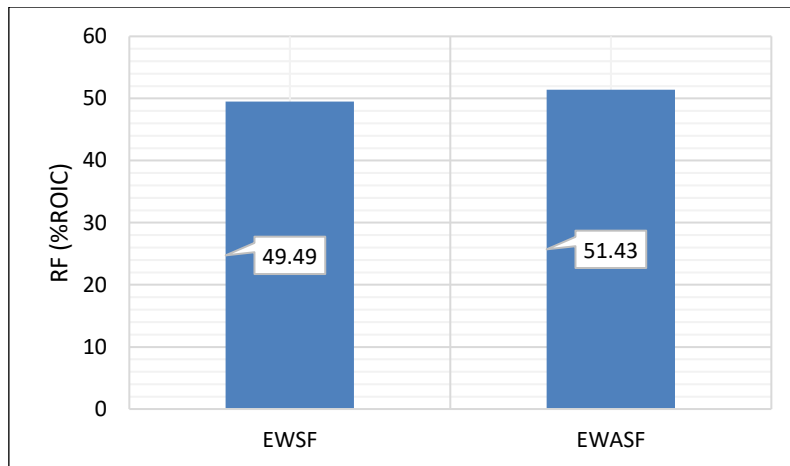


Figure 39. RF (%ROIC) for EWSF and EWASF core flooding experiments

Negative salinity gradient flooding designs were discussed in the methodology chapter. EWSF differs from the negative salinity flooding designs by the salinity of the used EW. The first negative salinity gradient concept flooding consists of two-step surfactant flooding with different salinity, so the salinity slope, in this case, is sharper. As Figure 40 illustrates, HSW recovered 41.26% of the oil. The oil recovery by this design was 66.40%, however, this negative salinity gradient has a total incremental oil recovery of 25.13%, which is higher than the conventional EWSF case.

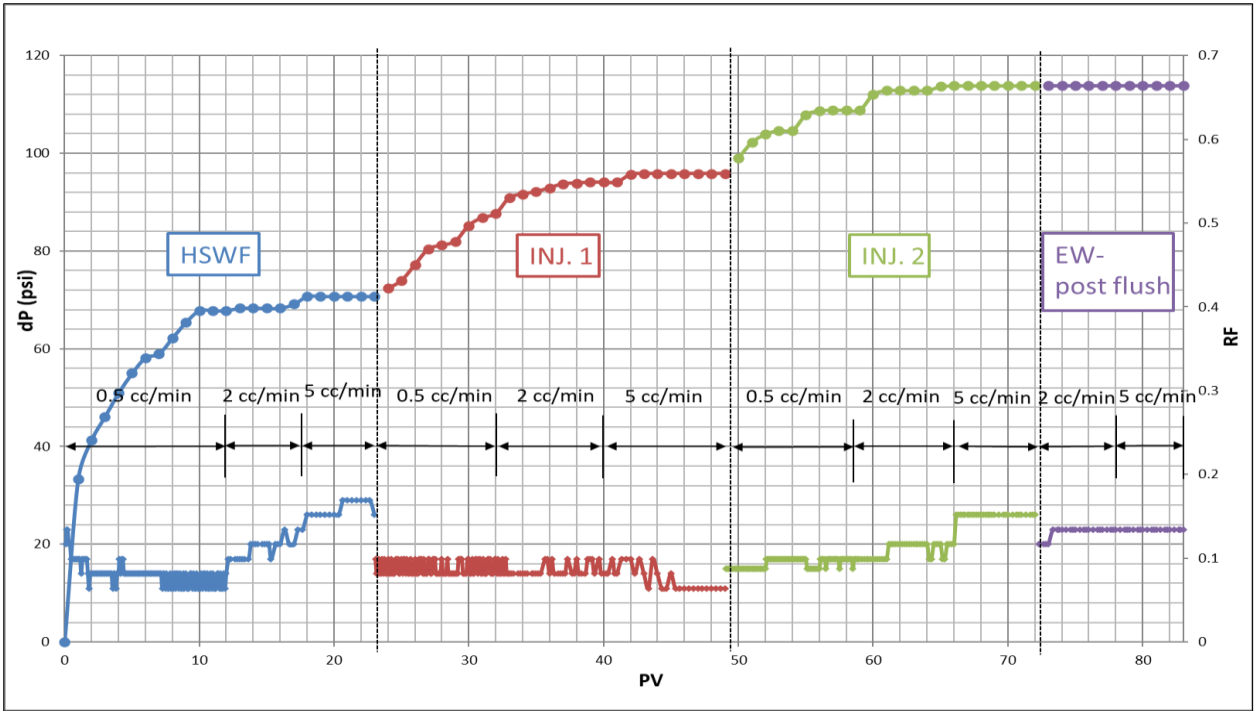


Figure 40. Negative salinity gradient experiment #3 results (dP and oil recovery vs PV injected)

The second negative salinity gradient flooding design has a gradual slope and consist of three surfactant flooding steps as Figure 41 presents. 38.79% of the oil was produced by HSW, Inj.1, Inj.2 and Inj.3 recovered 17.24%, 8.19% and 7.72% of incremental oil respectively.

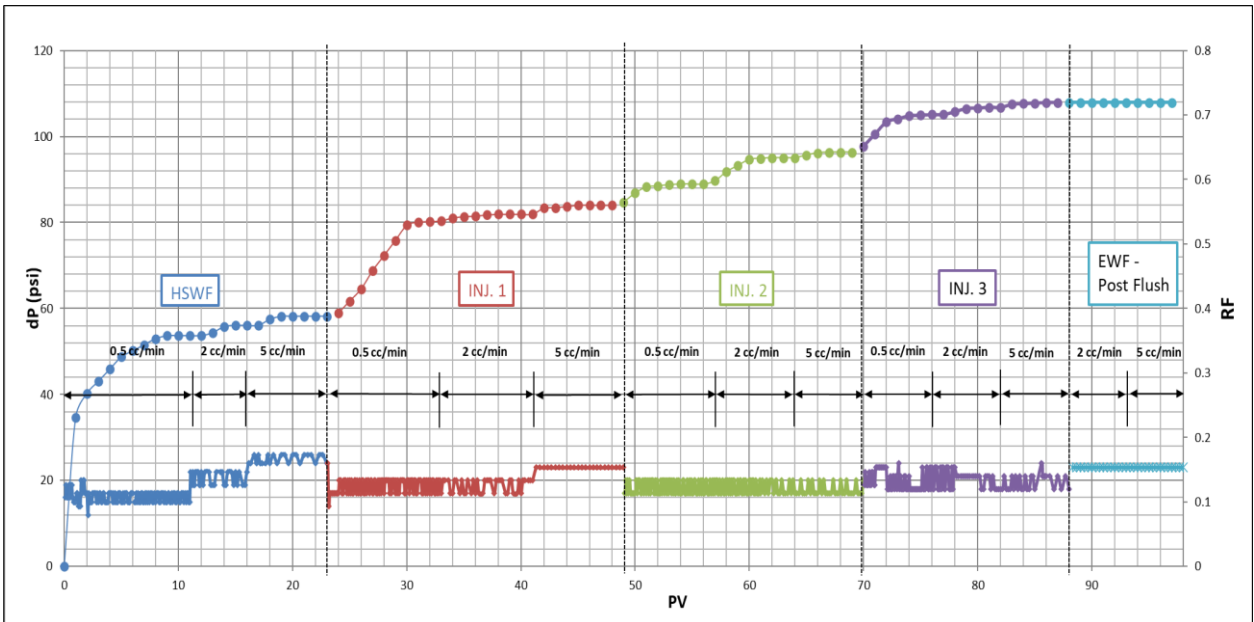


Figure 41. Negative salinity gradient experiment #4 results (dP and oil recovery vs PV injected)

Table 18. RF for Negative salinity gradient experiments

Process	Negative salinity gradient 1			Process	Negative salinity gradient 2		
	RF (%OOIC)	Inc. RF	RF (%ROIC)		RF (%OOIC)	Inc. RF	RF (%ROIC)
HSW	41.26		41.26	HSW	38.79		38.79
INJ. 1	55.89	14.63	24.9071526	INJ. 1	56.02	17.24	28.158
INJ. 2	66.40	10.5033534	23.8132644	INJ. 2	64.22	8.19	18.63
INJ. 3		-	-	INJ. 3	71.94	7.72	21.58
	Total	25.13			Total	33.14	

In terms of ROIC (%), Negative salinity gradient 2 shows the best performance compared to Negative salinity gradient 1 and EWSF flooding cases as presented in Figure 42.

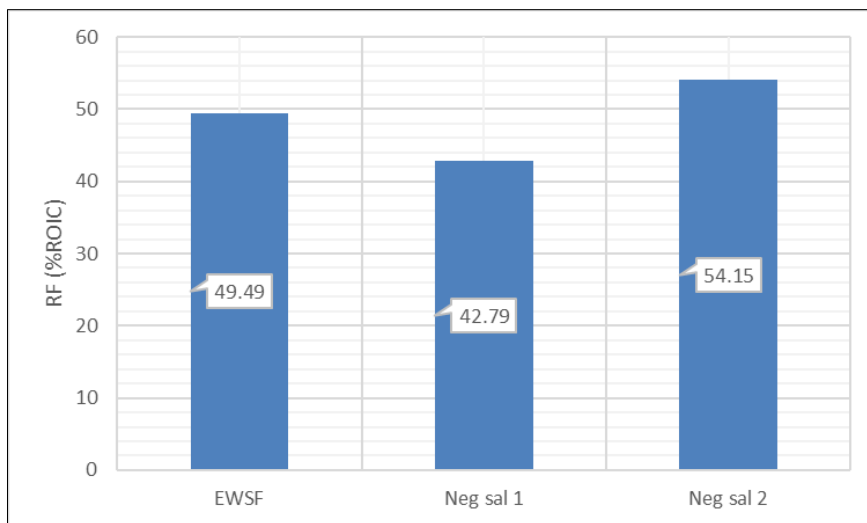


Figure 42. RF (%ROIC) for EWSF, Negative salinity gradient 1 and 2 core flooding experiments

Figure 42 shows that the application of negative gradient salinity can enhance the performance of the LSSF method and increases oil recovery. Hence the approach is recommended to be used in the design of the hybrid LSWF/SF EOR method in carbonates.

4 Conclusions and Recommendations

Hybrid CEOR evolving the synergy of the low salinity waterflooding and surfactant flooding has proved its effectiveness in carbonate cores. An experimental study shows that the performance of the method can be improved by the selection of an appropriate combination of the surfactant solution and the selected alkali (Na_2CO_3). It was shown that the application of alkali reduces the anionic surfactant adsorption on the carbonate surface and increases oil recovery. Moreover, the negative salinity concept was tested in limestone core samples and demonstrated promising results. Hence, by the experiments completed in this study, an effective design of the hybrid CEOR/LSWF was suggested. The following items are the main outcomes of the study.

- Aqueous stability, phase behavior, and static adsorption tests are the sufficient indicators to formulate the alkali/surfactant/engineered water mixture. The solution with 1 wt% of Soloterra 113H with the 1% of Na_2CO_3 prepared in 1.5 times diluted engineered water demonstrated the best results at 25 °C and 80 °C.
- The static adsorption test has demonstrated the utility of alkali (Na_2CO_3) on anionic surfactant adsorption on carbonates. The solution with 1 wt% of Soloterra 113H with the 1% of Na_2CO_3 prepared in 1.5 times diluted engineered water reduced surfactant adsorption from 1.02 mg/g rock to 0.15 mg/g rock.
- EASF coreflooding experiment revealed higher incremental oil recovery compared to EWSF which proves the benefit of the application of alkali in the CEOR design in the hybrid scheme. Three-step slightly sloped negative salinity gradient design showed higher incremental oil recovery compared to the conventional EWSF injection. This study suggests that the injection design and alteration in the salinity of the injected brines leads to better oil recovery due to the development of favorable phase behavior in the porous media..

Dynamic adsorption experiment may reveal better estimation of surfactant adsorption in a porous medium. These results may support the static adsorption data and oil displacement test results. Effluent ion analysis can help to improve the understanding of the mechanism behind the LSWF. To investigate the effect of utilization of cationic surfactant and alkali addition on adsorption on carbonate surface. This comparison can show if the cheaper way as alkali addition may provide the same low adsorption as cationic surfactant.

5 References

Abdallah, W., Buckley, J.S., Carnegie A., Edwards, J., Herold, B., Fordham, E., Arne, E., Habashy, T., Seleznev, N., Signer C., Hussain, H., Montaron, B., Ziauddin, M., (2007). Fundamental of wettability, Schlumberger, Oil field review.

Ahmed, S. and Elraies, K.A., (2018). Microemulsion in Enhanced Oil Recovery, Science and Technology Behind Nanoemulsions, Selcan Karakuş, IntechOpen, DOI: 10.5772/intechopen.75778. Available from: <https://www.intechopen.com/books/science-and-technology-behind-nanoemulsions/microemulsion-in-enhanced-oil-recovery>

Alagic, E. & Skauge, A., (2010). Combined Low Salinity Brine Injection and Surfactant Flooding in Mixed–Wet Sandstone Cores. Energy & Fuels. 24. 10.1021/ef1000908.

Alagic, E., Spildo, K., Skauge, A., & Solbakken, J. (2011) Effect of crude oil aging on low salinity and low salinity surfactant flooding. Journal of Petroleum Science and Engineering, 78:220–227. <https://doi.org/10.1016/j.petrol.2011.06.021>

Alameri, Waleed & Teklu, Tadesse Weldu & Graves, R. & Kazemi, Hossein & Alsumaiti, Ali. (2015). Low-salinity Water-alternate-surfactant in Low-permeability Carbonate Reservoirs. 10.3997/2214-4609.201412158.

Al-Yousef, H. Y., Lichaa, P. M., Al-Kaabi, A. U., & Alpustun, H., (1995). Wettability Evaluation of a Carbonate Reservoir Rock from Core to Pore Level. Society of Petroleum Engineers. doi:10.2118/29885-MS

Araz, A. and Kamyabi, F. (2015). Experimental Study of Combined Low Salinity and Surfactant Flooding Effect on Oil Recovery.

Austad, T., Strand, S., Puntervold, T., (2009). Is Wettability Alteration of Carbonates by Seawater caused by Rock Dissolution? International Symposium of the Society of Core Analysts held in Noordwijk, The Netherlands 27-30 September

Austad, T., Rezaeidoust, A., Puntervold, T., (2010). Chemical Mechanism of Low Salinity Water Flooding in Sandstone Reservoirs. SPE Improved Oil Recovery Symposium. 1. 10.2118/129767-MS.

Awolayo, A.N.; Sarma, H. K.; Nghiem, Long X., (2018). "Brine-Dependent Recovery Processes in Carbonate and Sandstone Petroleum Reservoirs: Review of Laboratory-Field Studies, Interfacial Mechanisms and Modeling Attempts" *Energies* 11, no. 11: 3020. <https://doi.org/10.3390/en11113020>

Bae, J.H., (1995)"Glenn Pool Surfactant Flood Expansion Project: A Technical Summary." *SPE Res Eng* 10: 123–128. doi: <https://doi.org/10.2118/27818-PA>

Bera, A., Mandal, A., (2014). Microemulsions: a novel approach to enhanced oil recovery: a review. *J Petrol Explor Prod Technol* 5, 255–268. <https://doi.org/10.1007/s13202-014-0139->

Buckley, J.S., (1995). Asphaltene precipitation and crude oil wetting—crude oils can alter wettability with or without precipitation of asphaltenes. *SPE Adv. Technol. Ser.* 3 (1), 53-59.

Chen H.L., Lucas L.R., Nogaret L.A.D., Yang H.D., Kenyon D.E., (2001), Laboratory monitoring of surfactant imbibition with computerized tomography, *SPEREE* (February), pp. 16-25

Chen J., G. Hirasaki, M. Flaum, (2006). NMR wettability indices: effect of OBM on wettability and NMR responses, *J. Pet. Sci. Eng.*, 52, pp. 161-171, 10.1016/j.petrol.2006.03.007

Al-Shalabi, E.W., Kamy Sepehrnoori, (2016). A comprehensive review of low salinity/engineered water injections and their applications in sandstone and carbonate rocks, *Journal of Petroleum Science and Engineering*, Volume 139, Pages 137-161, ISSN 0920-4105, <https://doi.org/10.1016/j.petrol.2015.11.027>.

Comelles, Francesc & Pascual, A., (1997). Microemulsions with butyl lactate as cosurfactant. *Journal of Dispersion Science and Technology - J DISPER SCI TECH.* 18. 161-175. 10.1080/01932699708943725.

Esene, Cleverson & Onalo, David & Zendejboudi, Sohrab & James, Lesley & Aborig, Amer & Butt, Stephen, (2018). Modeling investigation of low salinity water injection in sandstones and carbonates: Effect of Na⁺ and SO₄²⁻. *Fuel.* 232. 10.1016/j.fuel.2018.05.161.

Falode, O., & Manuel, E., (2014). Wettability Effects on Capillary Pressure, Relative Permeability, and Irreducible Saturation Using Porous Plate. *Journal of Petroleum Engineering*, 2014, 1–12. <https://doi.org/10.1155/2014/465418>

Fathi, S.J., Austad, T., and Strand, S., (2011). Water-Based Enhanced Oil Recovery (EOR) by “Smart Water”: Optimal Ionic Composition for EOR in Carbonates. *Energy & Fuels* 25 (11): 5173–5179.

Healy, R.N., Reed, R.L., Stenmark, D.G., (1976). Multiphase microemulsion systems. *SPEJ* (June), 147–160; *Trans. AIME*, 261. Huh, C., (1979). Interfacial tension and solubilizing ability of a microemulsion phase that coexists with oil and brine. *J. Coll. Int. Sci.* 71, 408–428.

Hiorth, A., Cathles, L.M. & Madland, M.V., (2010). The Impact of Pore Water Chemistry on Carbonate Surface Charge and Oil Wettability. *Transp Porous Med* **85**, 1–21
<https://doi.org/10.1007/s11242-010-9543-6>

Hirasaki, G.J., Miller, C.A., Pope, G.A., (2006). Surfactant based enhanced oil recovery and foam mobility control. 3rd Annual & Final Technical Report for DOE project (DE-FC26-03NT15406, July.

Hosseini, E., Chen, Z., Sarmadivaleh, M. et al., (2020). Applying low-salinity water to alter wettability in carbonate oil reservoirs: an experimental study. *J Petrol Explor Prod Technol* 11, 451–475 <https://doi.org/10.1007/s13202-020-01015-y>

Isabaev, et al., 2015. Chemical Composition and Properties of Formation Water, Oil and Gas. Herald of the Kazakh-British Technical University, pp. 72-78.

Johannessen, A. & Spildo, K., (2013). Enhanced Oil Recovery (EOR) by Combining Surfactant with Low Salinity Injection. *Energy & Fuels*. 27. 5738–5749. 10.1021/ef400596b.

Kamal, M.S., Hussein, A.I., Sultan A.S., (2017). Review on Surfactant Flooding: Phase Behavior, Retention, IFT, and Field Applications, *Energy & Fuels* 31 (8), 7701-7720, DOI: 10.1021/acs.energyfuels.7b00353

Kazankapov, N., (2014). Enhanced Oil Recovery in Caspian Carbonates with " Smart Water". In SPE Russian Oil and Gas Exploration & Production Technical Conference and Exhibition. Society of Petroleum Engineers.

Khanamiri H., Baltzersen Enge I., Nourani M., Stensen JÅ., Torsæter O., Hadia N., (2016). EOR by low salinity water and surfactant at low concentration: Impact of injection and in situ brine composition. *Energy & Fuel*. 30:2705-2713. DOI: 10.1021/acs.energyfuels.5b02899

Kokal, S., & Al-Kaabi, A.U., (2010). Enhanced oil recovery: challenges & opportunities. World Petroleum Council: Official Publication.

Kun Ma, & Cui, Leyu & Dong, Yezi & Wang, Tianlong & Da, Chang & Hirasaki, G. & Biswal, Sibani., (2013). Adsorption of cationic and anionic surfactants on natural and synthetic carbonate materials. Journal of colloid and interface science. 408. 10.1016/j.jcis.2013.07.006.

Lake, L.W., (1989). Enhanced Oil Recovery. Prentice-Hall.

Ligthelm, D.J., Gronsveld, J., Hofman, J., Brussee, N., Marcelis, F., van der Linde, H., (2009), Novel waterflooding strategy by manipulation of injection brine composition. In: EUROPEC/EAGE Conference and Exhibition. Society of Petroleum Engineers.

Liu, Shunhua, Li, Robert Feng, Miller, Clarence A., and George J. Hirasaki. (2010) "Alkaline/Surfactant/Polymer Processes: Wide Range of Conditions for Good Recovery." SPE J. 15, 282–293. doi: <https://doi.org/10.2118/113936-PA>

Marabayev N.A., Atchibayev A., Adayev Zh. (1999), Petroleum Encyclopedia of Kazakhstan, pp. 210.

McGuire P.L., Chatham J.R., Paskvan F.K., Sommer D.M., Carini F.H., (2005). Low salinity oil recovery: an exciting new EOR opportunity for Alaska's North Slope. In: SPE western regional meeting, Irvine, California, <https://doi.org/10.2118/93903-MS>.

McMillan, Marcia, D., Rahnema, H., Romiluy, J., Kitty, F.J., (2016), "Effect of exposure time and crude oil composition on low salinity water flooding", Fuel.

Meyers K.O., Salter S.J., (1980), The effect of oil brine ratio on surfactant adsorption from microemulsions. Presented at the SPE 55th annual fall technical conference and exhibition, Dallas, Texas

Murtada, H., & Marx, C., (1982), Evaluation of the Low Tension Flood Process for High-Salinity Reservoirs-Laboratory Investigation Under Reservoir Conditions. Society of Petroleum Engineers. doi:10.2118/8999-PA

Mwangi, Paulina Metili, (2010), An experimental study of surfactant enhanced waterflooding, https://digitalcommons.lsu.edu/gradschool_theses/2021

Nelson R.C., Pope G.A., (1978), Phase relationship in chemical flooding. Soc Pet Eng J 18:325–338

Nelson, Richard C., (1982). "The Salinity-Requirement Diagram - A Useful Tool in Chemical Flooding Research and Development." SPE J. 22: 259–270. doi: <https://doi.org/10.2118/8824-PA>

Novosad, J., (1982). Surfactant Retention in Berea Sandstone—Effects of Phase Behavior and Temperature. SPE J. 22 (6): 962–970. SPE-10064-PA. <https://doi.org/10.2118/10064-PA>.

Ottewill, R.H., (1984). Introduction. In: Tadros, T.F. (Ed.), Surfactants. Academic Press, pp. 1–18.

Pourafshary, Peyman & Moradpour, Nikoo., (2019). Hybrid EOR Methods Utilizing Low-Salinity Water. 10.5772/intechopen.88056.

Punternold, T., Austad, T., (2008). Injection of seawater and mixtures with produced water into North Sea chalk formation: impact of fluidrock interactions on wettability and scale formation. J. Pet. Sci. Eng. 63, 23-33.

Rao, D.N., (1996). Wettability effects in thermal recovery operations. SPE/DOE Improved Oil Recovery Symposium, 21-24 April.

Santanna, Vanessa & Castro, Tereza & Dantas Neto, Afonso., (2012), The Use of Microemulsion Systems in Oil Industry. 10.5772/36803.

Sekerbayeva, A., & Pourafshary, P., & Hashmet, M. (2020). Application of anionic Surfactant\Engineered water hybrid EOR in carbonate formations: An experimental analysis. Petroleum. 10.1016/j.petlm.2020.10.001.

Shariatpanahi, S.F., Strand, S., Austad, T., (2011). Initial wetting properties of carbonate oil reservoirs: effect of the temperature and presence of sulfate in formation water. Energy Fuels 25 (7), 3021-3028.

Shariatpanahi, S. F., Hopkins, P. H., Aksulu, S. Strand, T. Punternold,. Austad, T., (2016). "Water Based EOR by Wettability Alteration in Dolomite" , Energy & Fuels,

Sheng, James. (2015). Status of Surfactant EOR Technology. *Petroleum*. 79. 10.1016/j.petlm.2015.07.003.

Shimoyama, A., Johns, W.D., (1972). Formation of alkanes from fatty acids in the presence of CaCO₃. *Geochim. Cosmochim. Acta* 36, 87-91.

Solairaj, Sriram & Britton, Christopher & Kim, Do & Weerasooriya, Upali & Pope, Gary, (2012). Measurement and Analysis of Surfactant Retention. SPE - DOE Improved Oil Recovery Symposium Proceedings. 2. 10.2118/154247-MS.

Somasundaran, P., Agar, G.E., (1967). The zero point of charge of calcite, *Journal of Colloid and Interface Science*, Volume 24, Issue 4, 433-440.

Speight, J.G., (1999). *The Chemistry and Technology of Petroleum*. Chemical Industries. Marcel Dekker, New York, NY

Standnes, D.C., Austad, T., (2000). Wettability alteration in chalk. 1. Preparation of core material and oil properties. *J. Pet. Sci. Eng.* 28 (3), 111-121.

Strand, S., Hognesen, E.J., Austad, T., (2006). Wettability Alteration of Carbonates - Effects of Potential Determining Ions (Ca²⁺ and SO₄²⁻) and Temperature. *Colloid Surface A* 275(1-3): 1–10.

Stoeckenius W., Schulman J.H., Prince L.M., (1960). The structure of myelin figures and microemulsions as observed with the electron microscope. *Kolloid-Z* 169:170–178

Tahir, Muhammad & Hincapie, Rafael & Födisch, Hendrik & Abdullah, Hiwa & Ganzer, Leonhard. (2018). Impact of Sulphates Presence During Application of Smart Water Flooding Combined with Polymer Flooding. 10.2118/190796-MS.

Tang, G., & Morrow, N., (1999), Influence of brine composition and fines migration on crude oil/brine/rock interactions and oil recovery. *Journal of Petroleum Science and Engineering*, 24(2), 99-111.

Tavassoli S, Kazemi A, Korrani N, Pope GA., (2016), Low-salinity surfactant flooding—A multimechanistic enhanced-oil-recovery method. *SPE Journal*. 21(3):744-760. DOI: 10.2118/173801-PA

Teklu, T.W., Alameri, W., Kazemi, H., Ramona, M., Graves, AlSumaiti, A., (2017). Low salinity water–Surfactant–CO₂ EOR, *Petroleum*, Volume 3, Issue 3, 309-320, ISSN 2405-6561, <https://doi.org/10.1016/j.petlm.2017.03.003>.

Trushenski et al., (1974). S.P. Trushenski, D.L. Druben, D.R. Parrish Micellar flooding—fluid propagation, interaction and mobility *Soc. Pet. Eng. J.* (1974), pp. 633-642

Tuzhilkin, Katunin & Nalbandov, 2005. *Natural Chemistry of Caspian Sea Waters. The Caspian Sea Environment* , pp. 83-108

Webb KJ, Black CJJ, Al-Ajeel H., (2004). Low salinity oil recovery—Log-Inject-Log. In: SPE/DOE symposium on improved oil recovery, Tulsa, Oklahoma, 17–21 April 2004. <https://doi.org/10.2118/89379-MS>.

Wood, D.A., Yuan, B., (2018). Chapter Two - Low-Salinity Water Flooding: From Novel to Mature Technology, Editor(s): Bin Yuan, David A. Wood, *Formation Damage During Improved Oil Recovery*, Gulf Professional Publishing, 21-67, ISBN 9780128137826, <https://doi.org/10.1016/B978-0-12-813782-6.00002-6>.

Yousef, A. A., Al-Saleh, S. H., Al-Kaabi, A., & Al-Jawfi, M. S. (2011). Laboratory Investigation of the Impact of Injection-Water Salinity and Ionic Content on Oil Recovery From Carbonate Reservoirs. *SPE Reservoir Evaluation & Engineering*, 14(05), 578-593. doi:10.2118/137634-pa

Yousef, A. A., Al-Saleh, S., & Al-Jawfi, M. S. (2012). Improved/Enhanced Oil Recovery from Carbonate Reservoirs by Tuning Injection Water Salinity and Ionic Content. *Society of Petroleum Engineers*. doi:10.2118/154076-MS

Zhang, Y. and Morrow, N.R. (2006). Comparison of secondary and tertiary recovery with change in injection brine composition for crude oil/sandstone combinations. 2006 SPE/DOE Symposium on Improved Oil Recovery, Tulsa, Oklahoma, 22-26 April 2006, Paper SPE-99757. <http://dx.doi.org/10.2118/99757-MS>

Zhang Y, Xie X, Morrow NR. (2007). Waterflood performance by injection of brine with different salinity for reservoir cores. In: *SPE annual technical conference and exhibition*, Anaheim, CA, USA, 11–14 November 2007. <https://doi.org/10.2118/109849-MS>.

Zhou, Meifang & Rhue, R., (2000). Screening Commercial Surfactants Suitable for Remediating DNAPL Source Zones by Solubilization†. Environmental Science & Technology - ENVIRON SCI TECHNOL. 34. 10.1021/es9811546.

Ziegler, Victor M., and Lyman L. Handy.(1981) Effect of Temperature on Surfactant Adsorption in Porous Media." SPE J. 21 (1981): 218–228. doi: <https://doi.org/10.2118/8264-PA>

Zolotukhin A.B., Ursin J.R.,(2000). Introduction to petroleum reservoir engineering. Norwegian Academic Press, Høyskoleforlaget.